The Influence of Reactant Gas Solubility on Flooded Flow Fuel Cells

by

Levan F. Hiemke

Submitted to the Department of Mechanical Engineering
in partial fulfillment of the requirements for the degree of

Bachelor of Science in Mechanical Engineering

at the

MASSACHUSETTS INSTITUTE OF TECHNOLOGY

May 1991

Author .....
Department of Mechanical Engineering
May 20, 1991

Certified by .....
Jefferson Tester
Professor of Chemical Engineering
Thesis Supervisor

Accepted by .....
Professor Peter Griffith
Chairman, Thesis Committee

The Influence of Reactant Gas Solubility on Flooded Flow Fuel Cells

by

Levan F. Hiemke

Submitted to the Department of Mechanical Engineering
on May 20, 1991, in partial fulfillment of the
requirements for the degree of
Bachelor of Science in Mechanical Engineering

Abstract

This investigation focuses on the feasibility of a new concept in fuel cell design: the flooded flow fuel cell. The goal of this study and analysis of available literature was to determine if the solubility of hydrogen or oxygen in fuel cell electrolytes limits current density to unacceptable levels. A second goal of the analysis was to identify the electrolytes which have the best solubility characteristics.

This analysis clearly indicates that the solubility of hydrogen and oxygen in the electrolyte solutions of concern does not severely limit the current densities obtainable in flooded flow fuel cells. Trifluoromethane sulfonic acid (TFMSA) and sulfuric acid proved to be the least limiting as far as solubility is concerned. TFMSA also proved to be marginally feasible from a mass transfer limiting perspective. Obtainable current densities in potassium hydroxide and phosphoric acid, although not limited to unacceptable levels by oxygen solubility alone, were shown to be severely limited by oxygen mass transfer, which is a strong function of oxygen solubility.

Thesis Supervisor: Jefferson Tester
Title: Professor of Chemical Engineering

Acknowledgments

I greatly appreciate the help (*and patience!*) of Uli Holeshovsky and Jefferson Tester, who have introduced a small part of the world of chemical engineering to me. Without their help, it may have been a world that I would never have found.

Contents

List of Figures

List of Tables

Chapter 1

Introduction and Motivation

Fuel cells have the potential to become a major generator of electric power in the United States and worldwide. While their implementation has been primarily limited to the space program and a few terrestrial demonstration efforts, they are predicted to penetrate many markets during the 1990s. Should their performance be improved, their implentation would likely be further accelerated. The flooded flow concept is predicted to improve performance and could be a major contributor to the advancement of fuel cells. Several important technical questions must be answered before improvements from flooded flow fuel cells will be realized. This investigation addresses the issue of reactant gas solubility levels. These levels must be sufficiently high to support current densities which are superior to those found in standard fuel cells.

1.1 Conventional Fuel Cell Technology

The fuel cell is an electrochemical device which directly converts the chemical energy of a fuel and an oxidant into electrical energy. In this respect, fuel cells are similar to batteries; however, they differ from batteries in that they do not consume the materials that form an integral part of, or are stored within, their structure. The fuel cell is only a converter of energy.

The fuel cell consists of an ion conducting electrolyte sandwiched between a fuel

electrode, (the anode), and an oxidant electrode, (the cathode). A schematic diagram of the process by which a fuel cell generates electricity is illustrated in Figure 1-1; an expanded view of a basic fuel cell structure is displayed in Figure 1-2. A hydrogen-rich fuel enters the anode, which is coated with a catalyst, such as platinum. Upon contact, the hydrogen gas molecules dissociate into hydrogen ions and electrons. The hydrogen ions then pass through the electrolyte to the cathode. The electrons, however, can not pass through the electrolyte. Instead, they flow through a conductor connecting the anode to the cathode, thereby creating a current of electricity. The hydrogen ions and the electrons then react in the cathode with the oxidant to form water. Thus water and electricity are the end products of the electrochemical reaction.

Typical fuel cells produce high direct current in a low voltage of approximately 0.6-0.8 V. The associated power density is typically 1-2 kW/m^2 . In order to increase these values to a usable level, several fuel cells are connected in series in what is known as a stack. Stacks are then connected in parallel to provide the desired power. For large power plants, stacks of fuel cells can be mass produced in factories and assembled in parallel on-site. The maximum sized stack which can be transported by a truck from the factory to the power plant sites is approximately 10 MW [13].

A typical fuel cell power power plant consists of several systems. The major sections are a fuel processor, fuel cells, a power conditioner, and an energy recovery system. Other auxiliary systems include a water treatment system, a cooling system and a fuel storage system [13]. If the operating temperature of the fuel cell is low, the product water may enter the electrolyte. If this is the case, an evaporator or a reverse osmosis process may also be needed to avoid dilution of the electrolyte which would negatively affect performance [4]. A schematic diagram of a generic fuel cell power plant system is illustrated in Figure 1-3.

1.2 Attractive Characteristics of Fuel Cells

Fuel cells offer many benefits over conventional generators of electricity. The major benefits of fuel cells are high efficiencies, fuel flexibility, and ease of siting. Other

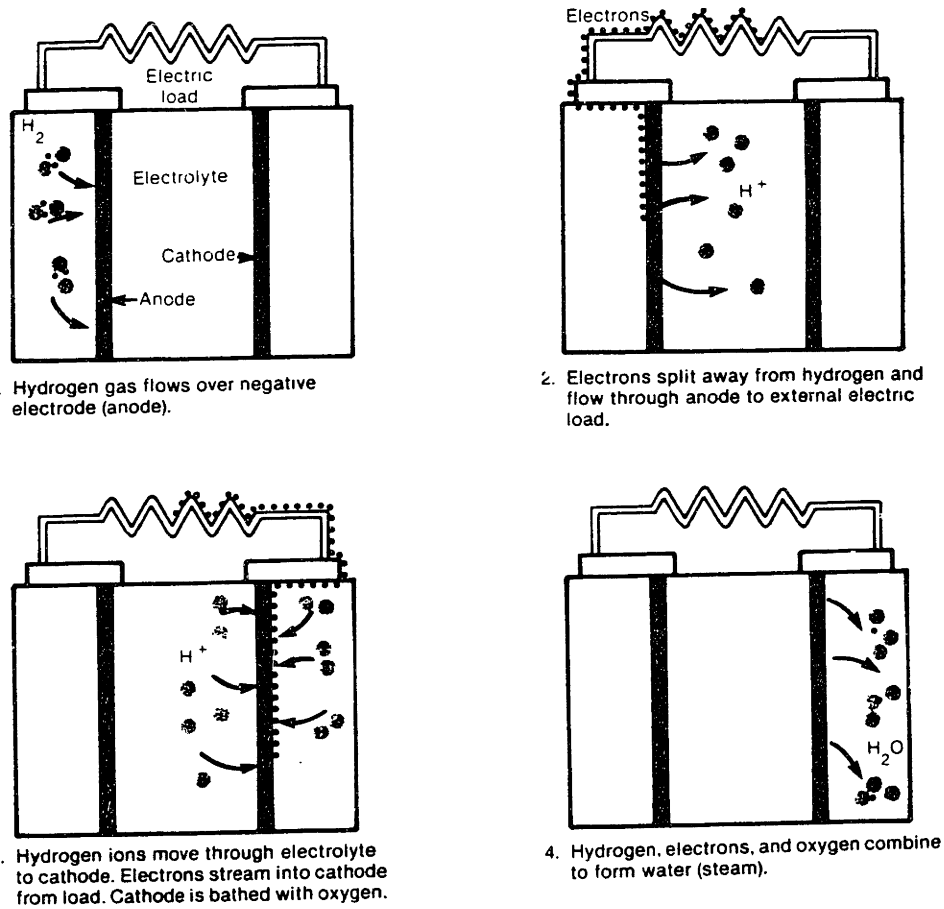

Source: Rala, 1984 [43]

Figure 1-1: Schematic diagram of the electrochemical process in a conventional (phosphoric acid) fuel cell

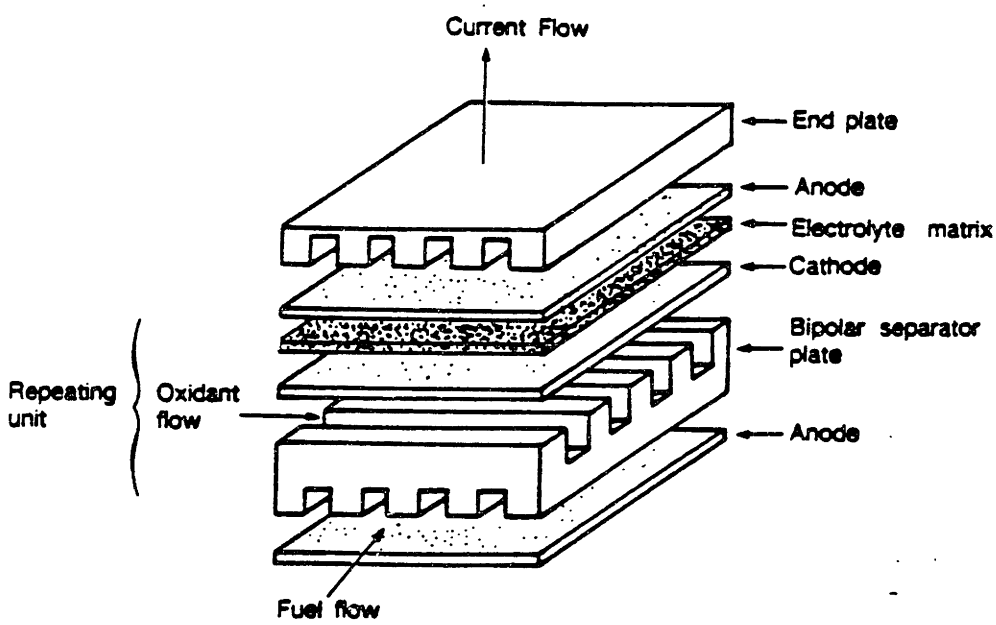

Source: Kinoshita, McLarnon, and Cairns, 1988 [31]

Figure 1-2: Expanded view of a conventional fuel cell structure

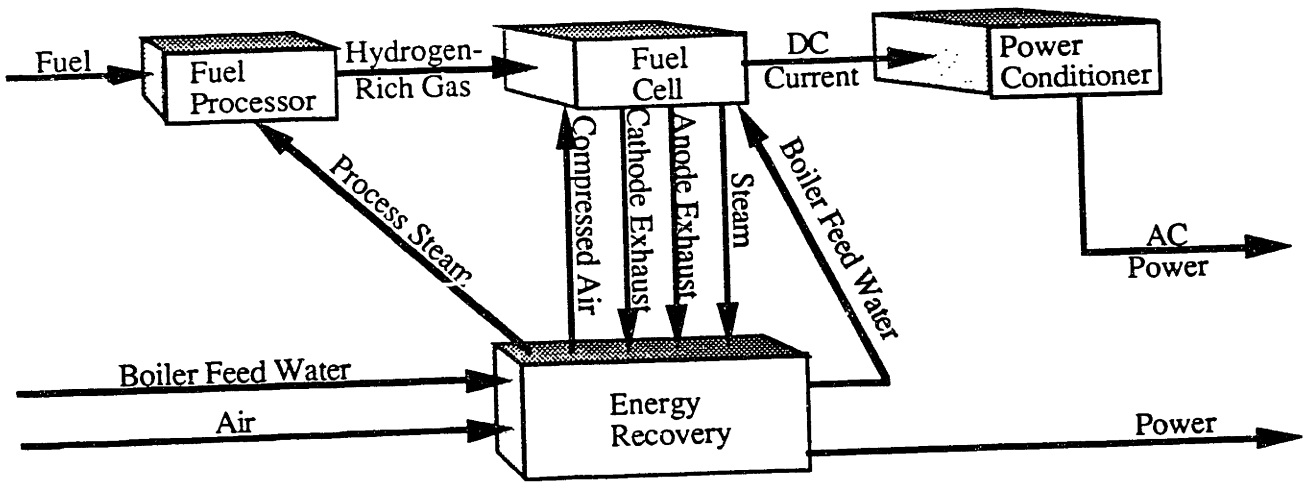

Source: Brown et al., 1985 [13]

Figure 1-3: Schematic diagram of a generic fuel cell power plant system

important features include excellent load following capability and mass producability.

1.2.1 High Efficiency

The high efficiency of the fuel cell is attributed to the direct conversion of chemical energy to electricity. "Fuel cells convert the free energy available from hydrogen molecules into electrical power by the electrolytic reaction of hydrogen and oxygen. This oxidation reaction is carried out in an isothermal environment, resulting in a very favorable conversion efficiency of fuel energy to electric power, substantially higher than the efficiency obtainable with conventional thermal cycles" [13, p. 2-2].

In an ideal electrochemical cell, all of the free energy is available as electrical energy; however, like heat to work converters, fuel cells can never reach their ideal efficiencies [4]. The theoretical efficiency of the fuel cell is 80 to 85 percent when the heat from the process is recovered [44]. The net fuel cell power plant efficiency is limited by the amount of energy necessary to convert a hydrocarbon fuel to a

hydrogen-rich fuel and by the efficiency of the power conditioner [13, 40]. The fuel cell can also maintain high efficiency through a range of 30 to 100 percent of rated output. Conventional power generation technology typically encounters major efficiency losses when output is below the full rated output.

1.2.2 Fuel Flexibility

Given the uncertain prices and supply of fuels, another attractive feature of the fuel cell is fuel flexibility. "In theory, any substance capable of chemical oxidation that can be supplied continuously (as a fluid) can be burned galvanically as the fuel at the anode of a fuel cell. Similarly, the oxidant can be any fluid that can be reduced at a sufficient rate" [4, p. 6]. The actual degree of fuel flexibility, however, is limited by the fuel processing technology used.

The two roles of the fuel processor are to convert the stock fuel to a hydrogen-rich gas and to remove impurities. The fuel processor must be specially designed for each fuel in order to eliminate contaminants which negatively affect performance. Commercially proven fuel processing technology exists in the petrochemical and petroleum industries for performing the task of converting a conventional fuel into a hydrogen-rich gas [13].

For economic reasons, natural gas and coal represent the principal fuels for fuel cell applications. However, the use of other fuels, such as biomass-derived ethanol, is technically feasible. According to Dr. San Martin, the Department of Energy's Deputy Assistant Secretary for Renewable Energy, "The use of fuels from biomass does not represent a major technical obstacle, but is more dependent upon competitive economics, the local fuel supply infrastructure, and uncertainties regarding capital costs and long-term durability" [24, p. 24]. Dr. San Martin further claims, "Once alternative fuels have been cleaned, switching fuels is a relatively low risk decision" [46, p. 18]. Thus, ethanol, while not an ideal fuel choice due to the low content of hydrogen, is one of many hydrogen-based fuels which could potentially be used in fuel cell applications. Some technical work is required in equipping fuel cells to handle different fuels, but for a large number of such fuels, the technical issues are

manageable. The economics, which includes the efficiency, of alternative fuels are the driving factors in determining the true fuel flexibility. Ethanol, for instance, may prove to only be competitive in remote areas with excess biomass.

1.2.3 Potential for Ease in Siting

Fuel cell power plants have characteristics which should allow them to be sited fairly easily. Fuel cell power plants have few moving parts and are therefore virtually noiseless. Air pollution, a major problem for urban siting of power plants, is minimal. "Because fuel cells do not rely on a fuel-burning process, their air pollution emissions are projected to be 1,000 to 10,000 times smaller than those of new fossil-fueled plants – even if the fossil plants employ the most advanced pollution control equipment" [50, p. 10].

Part of the decrease in air pollution emissions takes the form of reductions in the primary precursors to acid rain: nitrogen oxides and sulfur oxides. Nitrogen oxides are produced when nitrogen and oxygen interact at high temperatures. Since fuel cells operate at much lower temperatures than conventional combustion engines, NO_x emissions are much lower. Fuel cell power plants also emit much less sulfur oxides than conventional power plants.

Other pollutants are reduced as well. Hydrocarbon production is caused by incomplete combustion. The only combustion in a fuel cell power plant is in the auxiliary systems which produce warm gases which are recycled into the system. Thus, HC emissions are significantly lower. Since fuel cell plants run more efficiently than conventional fossil-fuel fired plants, they also emit less carbon dioxide per unit energy produced.

Thus, fuel cell technology has a significant advantage over conventional technology in environmental attractiveness. An environmental assessment of fuel cell technology jointly conducted by DOE and NASA concluded that "... sizable improvements in national air quality can be expected when fuel cells penetrate the energy supply market in substantial quantities" [40, p. 10]. These factors should enable fuel cell power plants to be sited in urban areas where electric power is needed most.

Fuel Cell Type	Anode Reaction	Transfer Ion	Cathode Reaction	Operation Temp. & Pressure
AFC	$H_2 + 2OH^-$ $\rightarrow 2H_2O + 2e^-$	OH^- $\leftarrow$	$\frac{1}{2}O_2 + H_2O + 2e^-$ $\rightarrow 2OH^-$	80-260°C 1-10 atm
PAFC	$H_2 \rightarrow 2H^+ + 2e^-$	H^+ $\rightarrow$	$2H^+ + O_2 + 2e^- \rightarrow H_2O$	30 – 250°C 1-8 atm
MCFC	$H_2 + CO_3^{2-}$ $\rightarrow H_2O + CO_2 + 2e^-$	CO_3^{2-} $\leftarrow$	$\frac{1}{2}O_2 + CO_2 + 2e^- \rightarrow CO_3^{2-}$	600 – 700°C 1-10 atm

Table 1.1: Electrochemical reactions and operational parameters for conventional fuel cells utilizing liquid electrolytes

1.3 Types of Conventional Fuel Cells

A variety of fuel cells are currently being pursued. A typical method of identifying the type of fuel cell is by the electrolyte employed, because the electrolyte largely dictates the operating conditions and composition of electrodes for achieving the required catalytic activity. Only fuel cells with liquid electrolytes are compatible with the flooded flow concept described in section 1.6 The three types of conventional fuel cells of interest are the alkaline fuel cell (AFC), the phosphoric acid fuel cell (PAFC), and the molten carbonate fuel cell (MCFC). The electrochemical reactions for these three fuel cells are shown in Table 1.1. Although similar in basic theory, the individual characteristics and engineering challenges vary significantly for each of these fuel cells.

1.3.1 Alkaline Fuel Cell Technology

Alkaline fuel cells were the first fuel cells to be used in real applications. They were used in the U.S. Gemini and Apollo Space Programs and are currently being used on space shuttles. The fuel cells used on space shuttles perform much better than those on the earlier programs. Selected performance parameters from these aerospace vehicles are presented in Table 1.2. Modern AFCs operate at temperatures of 80-90°C. AFCs typically use potassium hydroxide (KOH) for an electrolyte. The electrodes

Program	Current Density mA/cm^2	Mission Energy kWh (per module)	Mission Duration, h	Life h
Gemini	36	65	360	1000
Apollo	68	115	192	400
Shuttle	172	2600	168*	2000

* nominal
Source: Kinoshita, McLarnon, and Cairns, 1988 [31]

Table 1.2: Selected Performance Parameters from Aerospace Fuel Cells

are coated with catalytic substances such as platinum, palladium, and gold.

The major advantages of AFCs are excellent cathode performance due to rapid oxygen reduction kinetics and low materials cost [31, p. 105]. Furthermore, "it is estimated that the efficiency of AFCs on pure H_2 is about 60% [while] that of PAFCs is about 50%, based on the HHV of H_2" [31, p. 107]. A disadvantage to AFCs is that they do not reject carbon dioxide. As a consequence, they require pure hydrogen and oxygen for operation. This increases the cost of conventional alkaline fuel cells beyond a price which would be competitive for standard terrestrial applications. Without advancements which would significantly reduce their cost, AFCs will probably be used only at remote sites, such as in space, undersea, and military applications, which are not strongly constrained by cost.

State of the art AFCs use catalyzed carbon-based porous electrodes. The electrode performance indicates a dependence on the reactant gas concentration, with a higher polarization evident at lower concentrations. The performance of modern AFCs with carbon-based electrodes has not changed dramatically from that of earlier carbon-based electrodes. The major difference between the early cathodes and the modern cathodes is the limiting current for O_2 reduction from air has been improved [31].

The most recent advancement in AFCs was announced in 1987. United Technologies Corporation has developed an advanced lightweight system which features significant performance improvements. The fuel cell operates at 150°C and a partial pressure of 13.6 atm. At these conditions, it is capable of 1 A/cm^2 at 1.0 V, 5 A/cm^2

at 0.8 V, or 9 A/cm^2 at 0.72 V. This 90 kg system should be capable of providing 300 kW continuous power [4]. "The ongoing work in the alkaline fuel cell technology program is focused on increasing the life and power capabilities for future space shuttle operations. ...Future aerospace applications will require fuel cell systems capable of much greater power output than has been the case in the past" [4, p. 165].

1.3.2 Phosphoric Acid Fuel Cell Technology

Phosphoric acid fuel cells, until recently, were considered the most likely candidate for early commercialization in stationary power generation applications. They are the most mature of this class of fuel cells. They can be operated at temperatures as low as 35°C; however, current units are run at 200-250°C to eliminate polarization. PAFCs are constructed using an electrolyte of phosphoric acid in a matrix. The anodes of PAFCs are coated with platinum, which acts as a catalyst, to increase the rate of reaction.

While the present heat rates are approximately 8500 Btu/kWh, "... technology is sought which can be supplied to electric utilities at a capital cost of $1000/kW in quantity production and with a heat rate of 6900 Btu/kWh" [39, p. 22]. The DOE cost targets for natural gas-fueled systems are $800/kW for utility scale plants and $1300/kW for on-site units. The DOE cost target for coal-fired utility-scale plants is $1400/kW. The targeted efficiencies for utility-scale natural gas-fueled and coal-fueled systems are 45 to 50 percent and 40 to 50 percent, respectively [39].

Several companies are offering state-of-the art PAFCs. International Fuel Cells, a joint venture of United Technologies Corporation and Toshiba, has demonstrated a current density of 216 mA/cm^2 at an average cell potential of 0.73 V. UTC has designed an 11 MW system which would achieve a cell potential of 0.655 V at a current density of 216 mA/cm^2. Westinghouse has designed a system which would achieve a current density of 325 mA/cm^2 at 0.700 V. Engelhard Industries has been working on PAFCs which would use air as the oxidant. They have designed a system with a goal of achieving 161 mA/cm^2 at 0.68 V [4].

PAFC technology, though the most mature of the terrestrial fuel cell technologies,

still has some areas of uncertainty. The primary issue of uncertainty is the cost and reliability of components. A study conducted for EPRI "...demonstrates that the limiting factor for multi-megawatt PAFC power systems is the development of the fuel cell stacks and solid state power converter" [13, p. 12-1]. Another issue of concern in the long run is energy security. This technology relies upon the use of platinum as a catalyst. Since more than 90% of the United States's supply of platinum is imported from unstable regions of the world (South Africa and the Soviet Union), this would force reliance upon unstable external sources of platinum and potentially endanger the nation's energy security.

1.3.3 Molten Carbonate Fuel Cell Technology

Molten carbonate fuel cells are believed by many to be the stationary application fuel cell technology of the future (mid-1990s and beyond). MCFCs are constructed using an electrolyte of lithium and potassium carbonates. They are operated at 600-700°C to keep adequate ionic mobility, or conductivity, in the electrolyte. An effect associated with this higher temperature is that a less active catalyst is required; therefore, expensive noble metal catalysts such as platinum can be avoided. Another advantage of high temperature operation is increased cogeneration capabilities due to the high quality waste heat. This high temperature also enables internal fuel reforming; an external fuel processor is not required as methane (natural gas) can be catalytically converted to hydrogen in the anode compartment. For this reason, MCFCs should be more fuel flexible than PAFCs.

MCFCs should also have a more attractive heat rate than PAFCs. It is believed that molten carbonate heat rates may be reduced to as little as 5900 Btu/kWh [40]. In addition, MCFCs are able to operate above their rated capacity with only a small decrease in efficiency. The DOE cost targets for natural gas-fueled systems are \$600/kW for utility scale plants and \$1100/kW for on-site units. The DOE cost target for coal-fired utility-scale plants is \$1200/kW. The targeted efficiencies for utility-scale natural gas-fueled and coal-fueled systems are 55 to 60 percent and 50 to 55 percent, respectively [39]. Typical MCFCs are expected to operate at a current density of about 200

mA/cm^2 at a unit cell voltage of more than 0.8 V under pressurized conditions [4].

Control of contaminants in MCFCs is the major technological challenge facing engineers who are developing the technology. Carbonate poisoning of the reforming catalyst is a problem. This contributes to a limited life expectancy of the fuel cell stacks. Other factors limiting stack life include the stability of the nickel-oxide cathode and sintering and creep problems of the anode. The current stack life is approximately 10,000 hours; the targeted stack life is 40,000 hours.

1.4 Commercial Opportunities for Fuel Cells

In the coming years, fuel cells are expected to find many opportunities in the commercial sector. Since fuel cells are very flexible, they will likely find a number of different applications.

1.4.1 Applications of Fuel Cells

A number of varied applications exist for the different types of fuel cells. The primary potential market sectors include electric utility generation, independent power production, industrial cogeneration, on-site commercial cogenration, aerospace and military applications, residential cogeneration, and tranportation [53]. A list of potential applications, the corresponding market sizes, the appropriate fuel cell types, and approximate fuel cell sizes are exhibited in Table 1.3. The need for new large-scale electric power generating capacity could be decreased or postponed by several fuel cell applications. These applications are specified in Table 1.4. Note that these tables also include fuel cells with non-liquid electrolytes which are not applicable to the flooded flow concept.

The electric utility industry hopes to use fuel cells for peak-shaving, load following, and eventually, baseload power plants [40]. Potential industrial applications include municipal waste treatment plats, breweries, paper mills, petroleum refineries, metal refining, and chlor-alkali production. Potential on-site commercial sector applications include apartment buildings, office buildings, restaurants, motels, hotels, hospitals,

Editor's Note: The following table was taken from "Fuel Cells Workshop Proceedings—Potential Opportunities in Canada," dated April 28, 1988, Toronto, Canada, and issued by the Ontario Ministry of Energy. This document is available through this Ministry, see the September 1988 issue of FCN for details. The following is a key to the abbreviations used in the table: US—United States, CAN—Canada, ONT—Ontario, BC—British Columbia, NG—Natural Gas, LNG—Liquified Natural Gas, H_2—Hydrogen, HC—Hydrocarbon, Me—Methanol, O_2—Oxygen)

MARKET SEGMENT	TYPICAL SYSTEM SIZE	MARKET SIZE, MW	PREFERRED FUEL	COMPETITIVE ADVANTAGE
Spacecraft	1 50 kW	1	H_2/O_2	Compactness, energy/weight ratio Source of drinking water
Energy Systems Electric Utility	1-20 MW	17,500 (US) 2,000 (ONT)	NG, OIL COAL	Short construction time, Modularity, Expandability, Distributed power generation, Clean operation in urban areas
Cogeneration, Commercial and Residential Buildings	25-1000 kW	18,000 (US) 4,000 (ONT) 412 (BC)	NG	Use of by product heat, Lowering peak demand
Northern Ontario Communities	0 1-1 2 MW	10	OIL, LNG H_2	Use of by product heat, Better fuel utilization
Remote communities in Quebec	0 1-1 MW	100	OIL/LNG H_2	Ditto
Industrial Generation/Cogeneration Chloralkali/chlorate	0 5-10 MW	2,975 (US) 300 (CAN)	H_2	Utilization of by-product H_2, Lowering electricity demand
Petrochemical	5 MW	4,500 (US) 172 (BC)	H_2, HC	Ditto
Petroleum Refining	5 MW	12,000 (US) 36 (BC)	H_2, HC	Ditto
Resource Industries: Underground Mining	20-500 KW	500 (CAN)	H_2	Low pollution underground, Low noise, Low waste heat, Elimination of 600V grid
Wood Product Mills	1 MW	164 (BC)	NG	By product heat cost
Pulp and Paper Mills	5 MW	252 (BC)	NG	Ditto
Metal Mills (aluminum)	5 MW	93 (BC)	NG	Ditto
Other Industries: Malt Beverage, Food	500 kW	65 (BC)	NG	Ditto
Commercial and Military Stationary Generators Military, Coast Guard, Remote Site—Weather, Communications Backup Power—Computer, Communications Emergency Power—Mines, etc.	0 5-500 kW	10,000	NG, Me, H_2, LNG	Fast start, Low noise and emissions
Portable Generators	0.1-7 kW	15,200	Me, H_2, LNG	Self-starting, Instant start, Clean and quiet operation
Consumer Products for outdoors, RV's, cottages, households, education, hobbies	0.1-5 kW	open	Me, H_2	Operational characteristics unattainable with batteries or internal combustion engines
Transportation Railway Locomotive	2.5 MW	48,000 (US) 7,500 (CAN)	H_2, LNG, Me, OIL	Electrification via fuel cell, Elimination of need for overhead catenary
Ships	1-5 MW		H_2, LNG, ME	
Submarines, small submersibles	10-750 kW	0.2 (CAN)	$H_2.O_2$	No exhaust-full submerged operation on hydrogen
Heavy trucks, Buses	260 kW	36,400 (CAN)	Me, H_2	Environmentally clean, Efficient-better mileage
Vans and automobiles	10-40 kW	175,000 (CAN)	Me	Ditto
Specialized vehicles -forklift trucks -golfcarts -wheelchairs, -etc.	1-10 kW	6,000	Me, H_2	Clean and efficient possible indoor operation, Lower cost and better operational characteristics than on batteries

Source: Fuel Cell Association, 1989 [5]

Table 1.3: Potential markets for fuel cells

Use	Energy Source[a]		Energy range, kW
	Combustion Fuel	Fuel Cell	
Portable-power cordless chargers	MeOH, H_2 (bottle)	AFC, PAFC, MeFC	0 05–5
Stand alone	Biogas, landfill gas, producer gas	PAFC, MCFC, AFC (H_2SO_4)	1–100
UPS standby	MeOH, EtOH, H_2	AFC, MeFC, SPE	1–100
On-site/integrated energy systems	Natural gas, SNG	PAFC, MCFC, SOFC	50–1200
Cogeneration plants	Natural gas, SNG, others	MCFC, SOFC	1000–10,000
Dispersal power plant	Natural gas, SNG, others (solid fuel)	PAFC, MCFC, SOFC	10,000–100,000
Central power plants	Coal, biomass, residual oils	MCFC, AFC, SOFC	100,000–500,000

[a] AFC, alkaline fuel cell; MCFC, molten carbonate fuel cell; MeFC, direct methanol fuel cell, PAFC, phosphoric acid fuel cell; SNG, synthetic natural gas, SPE, solid polymer electrolyte fuel cell, UPS, uninterruptible power supply

Source: Lindstrom, 1989 [34]

Table 1.4: Stationary Electric power applications

and airports. The characteristics targeted by the DOE for PAFCs and MCFCs for electric utility, industrial, and on-site applications are displayed in Table 1.5. Since fuel cell power plants are able to operate unmanned, they are a logical candidate as the main power source for remote siting applications for military operations such as the Alaskan Air Commands Minimally Attended Radar Sites on the Defense Early Warning (DEW) line [24]. The recent development of a thin-film fuel cell introduces a new area of applications ranging from low-cost, small, lightweight fuel cells as high use battery replacements to new applications in information processing [21]

The fuel cell also functions well as a complement to a renewable energy source such as solar or wind power. Off-peak electricity production from renewables can be used to produce hydrogen by an electrolysis process. This hydrogen can be stored and utilized in fuel cells as an additional power source during peak periods, thereby enhancing the renewable system's spinning reserve and load-following capability.

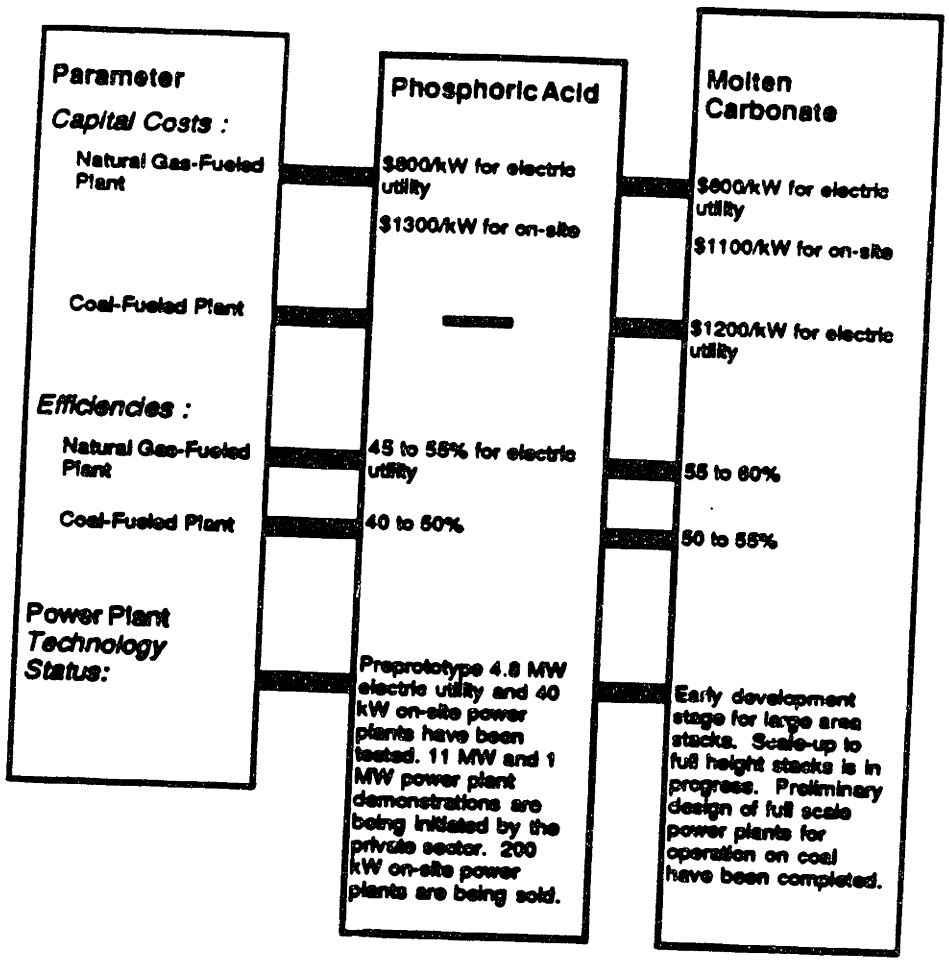

* Power plant costs are in FY1990 dollars and efficiencies are based on the higher heating value of fuels. Efficiencies are for production of electricity only; the amount of additional thermal energy available in cogeneration will be dependent on the application.

Source: US DOE, 1989 [39]

Table 1.5: Fuel cell characteristics targeted by the Department of Energy

1.4.2 Domestic Market

According to a joint analysis by the DOE and the DOD, "The analyses indicate that at the initial commercial market prices, fuel cells will be economically attractive at many facilities in the United States" [24, p. 99]. The actual level of attractiveness of a natural gas fueled fuel cell power plant is largely dictated by the regional price of natural gas versus electricity. The uncertainty of fuel prices as well as other uncertainties prevent accurate quantitative evaluations from being made. Swedish fuel cell expert, Olle Lindstrom, made this point in claiming that "... at present, quantitative estimates should not be taken seriously" [34, p.50]. However, they do provide some degree of insight into the future of fuel cell applications.

"Most markets for new products develop around a niche that can place a high value on the new product's features. This higher valuation is necessary because higher cost or higher risk to the buyer usually accompanies early market products" [23, S-5]. Predictions related to what market sector will fulfill this "niche" characterization and become the first market for fuel cells vary dramatically. According to a study by the American Public Power Association, "In both characterizing and quantifying the market for fuel cells, it is clear that public power represents possibly the best early market for fuel cells" [23, S-5].

M-C Power Company's market analyses agree that "initial applications in the utility sector ...will be for 'dispersed' generation in urban and suburban areas using systems less than 10 MW in size" [15, p. F-43]. However, they also believe that the early niche market will not be the utility sector, but rather, that "the commercial sector will be the most attractive for near term applications" [15, p. F-47]. A summary of their minimum market projections for the period from 1990 to 2000 is displayed in Table 1.6.

A.J. Appleby and F.R. Foulkas, fuel cell experts from academia, disagree with both of these predictions. They claim, "The first commercial fuel cells will almost undoubtedly be multi-megawatt units that will cost hundreds of millions of dollars to construct. Smaller units for special applications will probably follow" [4, p. 14]. Much of this will depend upon the efforts made by all of those involved with fuel cells

	COMMERCIAL		INDUSTRIAL		UTILITY		TOTAL	
Type of Fuel Cell	Demo Units	Comm Units	Demo Units	Comm Units	Demo Units	Comm Units	Demo Units	Comm Units
PAFC	10	100	30	60	60	100	100	260
MCFC	10	10	10	20	20	160	40	190

Source: Camera & Schora, 1990 [15]

Table 1.6: Minimum Estimated Market (in MW) for Demonstration and Commercial Fuel Cells, 1990-2000

to expedite commercialization.

On-Site Fuel Cell Power Plant Markets

The Gas Research Institute has estimated the size of the commercial market for fuel cells. They claim that the U.S. commercial sector represents approximately 4 million sites and approximately 175,000 MWe of cumulative peak demand. If a $1000/kw installed cost is realized, an economically feasible market of 18,000 MW results [53]. These are the same results cited in an earlier study by the Onsite Fuel Cell Users Group [26, p. 1-9]. This study also assessed the market potential for grid-connected on-site units. "If the current favorable legal/regulatory environment continues to exist, the economically feasible market for Onsite fuel cells at $1000/kW and operating in the grid-connected configuration would approach 68,000 MW of installed capacity." Additionally, "even at installed costs of $3000/kW, a substantial market opportunity – approximately 12,000 MW – for grid-connected operation exists" [26, p. 1-8 – 1-9].

Utility-Scale Fuel Cell Power Plant Markets

Private utilities are currently hesitant about taking a chance with a new technology such as the fuel cell; however, public utilities may, in contrast, comprise an attractive early market. The American Public Power Association has attempted to quantify a market for fuel cell power plants. The market that they have analyzed is the publicly owned power generating sector. Public power applications, though representing only about 14% of the electric utility industry, appear to have great potential for fuel cell use. Public power is an attractive application for fuel cells for many reasons, includ-

ing potential transmission constraints, environmental constraints, and an interest in increased self reliance. These factors, among others allow public power planners to justify paying more than traditional economic analyses would suggest. "Public power is the largest potential market for fuel cells and it may be the most accessible early market" [23, S-5].

"We have identified about 100 utilities representing nearly 5 million customers (a third of all customers served by public power systems) that may be characterized as our 'likely early' market for fuel cells. Their total requirements for capacity additions average about 650 MW each year. The median-sized entity in this likely early market would need to add about 4.5 MW in capacity every 3 years" [10, p. 4]. Once the public power market opens up, the private market should begin to open up as well.

Integrated Renewable Energy-Fuel Cell Markets

Another market which may prove to be quite large is the complementary renewable energy-fuel cell systems market. Fred Sissine, the Congressional Research Service's fuel cell expert, claimed in an independent report that "...an integrated renewable energy-fuel cell system could compete initially for the 10,000 megawatt (MW) market for stand-alone power systems in rural areas and developing countries, where the primary competition would be stand-alone diesel power and wind-diesel power systems" [49, p. 1].

In a CRS report, Mr. Sissine claimed, "The combined output of these complementary facilities may enable them jointly to defer or displace some conventional power plant construction before the year 2000" [50, p. 6]. General application fuel cell market-expansion also may occur as a side benefit of the use of fuel cells in this manner. "The development of renewable energy-fuel cell systems might expand markets for both fuel cells and renewable power technologies. With expanding markets, increased production volumes would likely reduce unit costs for both technologies. Lower unit costs could further expand the markets and improve the competitiveness of U.S. equipment in domestic and foreign markets" [49, p.6].

1.4.3 International Market

The diverse characteristics of fuel cells enable application in many international markets. India has expressed interest in fuel cells since 1979. Based on a capital cost of $1000/kW, India has determined that the total potential market for PAFCs in India is substantial. The market for natural gas-fired units is about 500 MW; the market for units fueled by molasses-derived ethanol is about 500 MW; and the market for units fueled by biogas from anaerobic digestion is about 3000 MW. In Argentina, "... fuel cell generators at a 2500 US$/kw capital cost should have, at least, a 600 MW market for systems in the 20 kW - 200 kW range" [36, 312]. Many other foreign markets exist and need to be assessed.

1.5 Near-Term Prospects for Fuel Cells

The fuel cell is a highly attractive power generation option for the 1990s and beyond. The fuel cell is based on fairly simple technology, with more advanced concepts being utilized to improve its operation. A significant market for fuel cells appears to exist. This market has prompted extensive research efforts by the United States, Japan, and many other countries. Commercialization efforts, however, have been rather limited. Only Japan has successfully embarked on a moderate-scale commercialization effort. The United States government has been involved in fuel cell efforts for the past three decades. The role of the federal government has evolved over time as it has met with a myriad of fuel cell technology and policy issues related to fuel cells.

In a recent editorial in Science, Philip H. Abelson remarked, "Prospects are that in the coming decades, fuel cell technology will have a large role in global energy production" [2, p. 1469]. One of the reasons for such optimism is the fact that the federal government, (particularly the legislative branch), favors fuel cell technology. According to Rita A. Bajura of the DOE's Morgantown Energy Technology Center:

> DOE is attempting to accelerate the commercialization of the fuel cell technology. We are trying to push the technology out of the R&D phase

and into the demonstration plant phase and position the technology so that it can be commercialized by the private sector. The question is, why accelerate? The answer is that we think DOE's strategy to accelerate commercialization has benefits. I see two benefits. The first benefit deals with maintaining U.S. industrial competitiveness. Acceleration will help to protect the potential market share of U.S. fuel cell manufacturers. Acceleration of commercialization is a world-wide phenomenon: The time frame to move a product from the R&D lab to the consumer is shortening. ...If U.S. manufacturers do not commercialize fuel cells as rapidly as possible, our country will lose its technological edge in fuel cells, and non-U.S. groups will take over the commercialization efforts. The second benefit is that we will have a more cost-effective research program, thus saving the taxpayers money, by identifying the real issues earlier in the program. We need to get the technology out of the R&D laboratory and into the demonstration phase to learn what the real technical roadblocks are, and then to solve them" [6, p. 6].

1.6 The Flooded Flow Fuel Cell Concept

The flooded flow fuel cell concept, proposed by the late Prof. Herman P. Meissner of MIT's Chemical Enginnering Department [37], in theory, could improve the efficiency at which fuel cells with liquid electrolytes operate. In his doctoral thesis proposal, Uli Holeshovsky has proposed several different configurations for operating flooded flow fuel cells [29].

Conventional fuel cells utilize porous gas diffusion electrodes which have a high "internal" surface area to "external" surface area ratio, where the "internal" surface area refers to the surface area of the pores and the "external" surface area refers to the area of the faces of the electrode. It is widely accepted that the electrochemical reactions which take place in a conventional fuel cell occur only at a narrow band within the pores where the catalyst-coated electrolyte is in contact with both the reactant gas and the electrolyte. Since the reactions only take place at the meniscus of the gas-electrolyte interface, most of the internal surface area is not involved with the electrochemical reaction at a given instant in time. The flooded flow concept would enable the fuel cell to make use of all of the internal surface area, as well as the external, electrode surface area.

Flooded flow implies that the electrolyte is saturated with the reactant gas and then circulated through the electrode. As the gas-electrolyte mixture flows through the electrode, and over its faces, the gaseous solute molecules will react when they come into contact with the electrode. Since the electrolyte will be present over the entire electrode, the effective surface area will be the sum of the internal and the external surface area of the electrode.

1.6.1 Flooded Flow Operation

Two separate configurations have been proposed for flooded flow operation: the separate feed and the mixed feed system. The separate feed system is simpler, but would likely be more expensive than the mixed feed system. However, the mixed feed system has some unique uncertainties which must be addressed.

The separate feed system, schematically shown in Figure 1-4, includes an ion exchange membrane which separates the anolyte (the hydrogen-saturated electrolyte) from the catholyte (the oxygen-saturated electrolyte). Hydrogen and oxygen are individually saturated in electrolyte solutions in a stoichiometric ratio of 2 to 1. The anolyte is pumped through the anode; the catholyte is pumped through the cathode. The electrolytes are then repurified and recycled back into the saturators.

The rate of electrochemical reaction in the separate feed configuration can be controlled to some extent by varying the velocity of the gas-electrolyte mixtures. It may also be possible to pump the two mixtures at different velocities, and thereby alter the ratios from the stoichiometric 2 to 1 ratio. It also may be possible to utilize two different electrolyte solutions if it is desired.

With the mixed feed configuration schematically shown in Figure 1-5, the gases are once again individually saturated in electrolyte solutions; however, the anolyte and catholyte are then mixed together resulting in an electrolyte solution which is saturated with both hydrogen and oxygen. This mixed electrolyte is then pumped across both the anode and the cathode. It is hoped that the gases will react selectively at the anode and the cathode and that shunt currents will be minimal. The spent electrolyte is then repurified and recycled back into the two saturators.

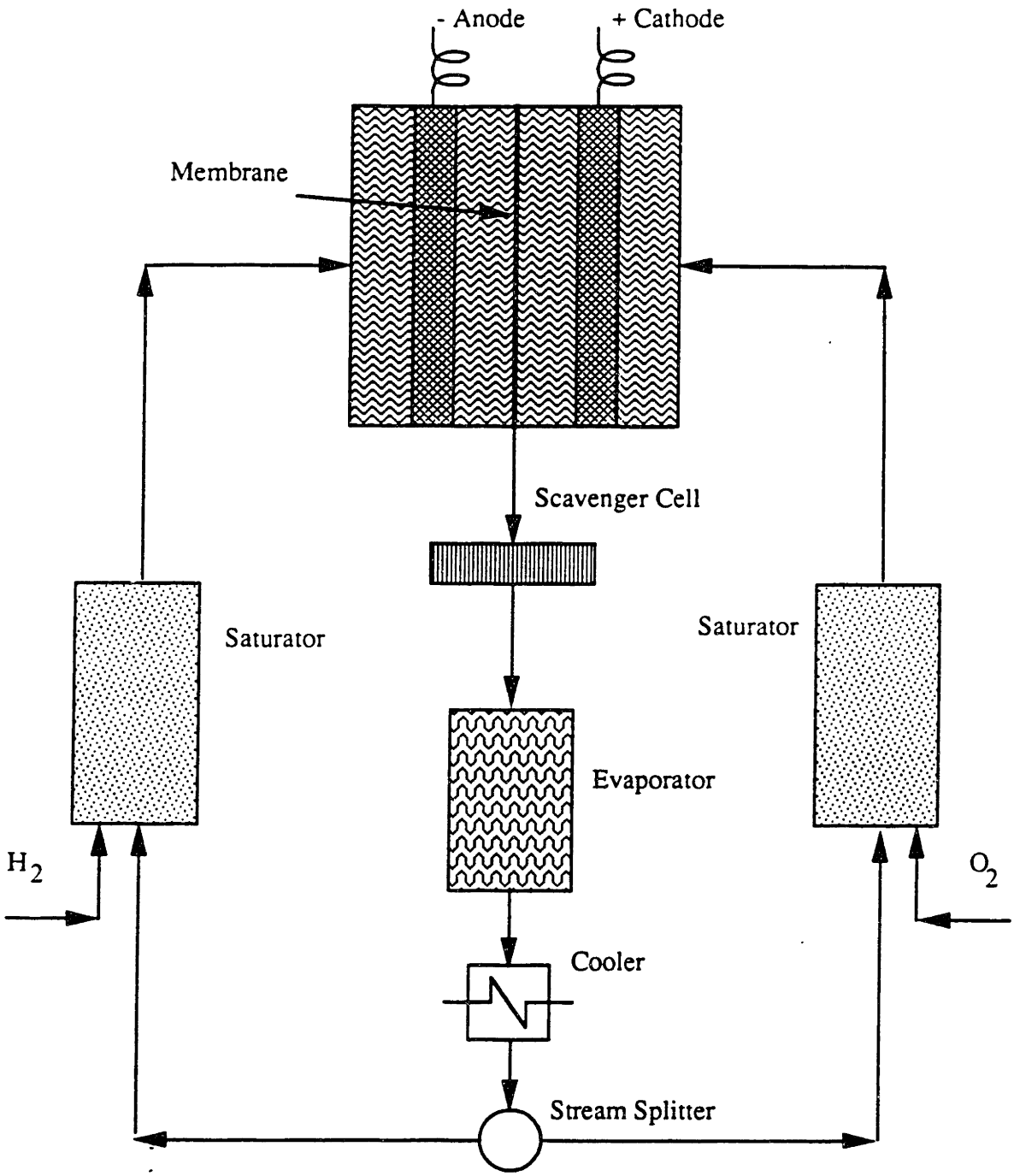

Source: Holeschovsky, 1991 [29]

Figure 1-4: Schematic diagram of a separate feed flooded flow fuel cell system

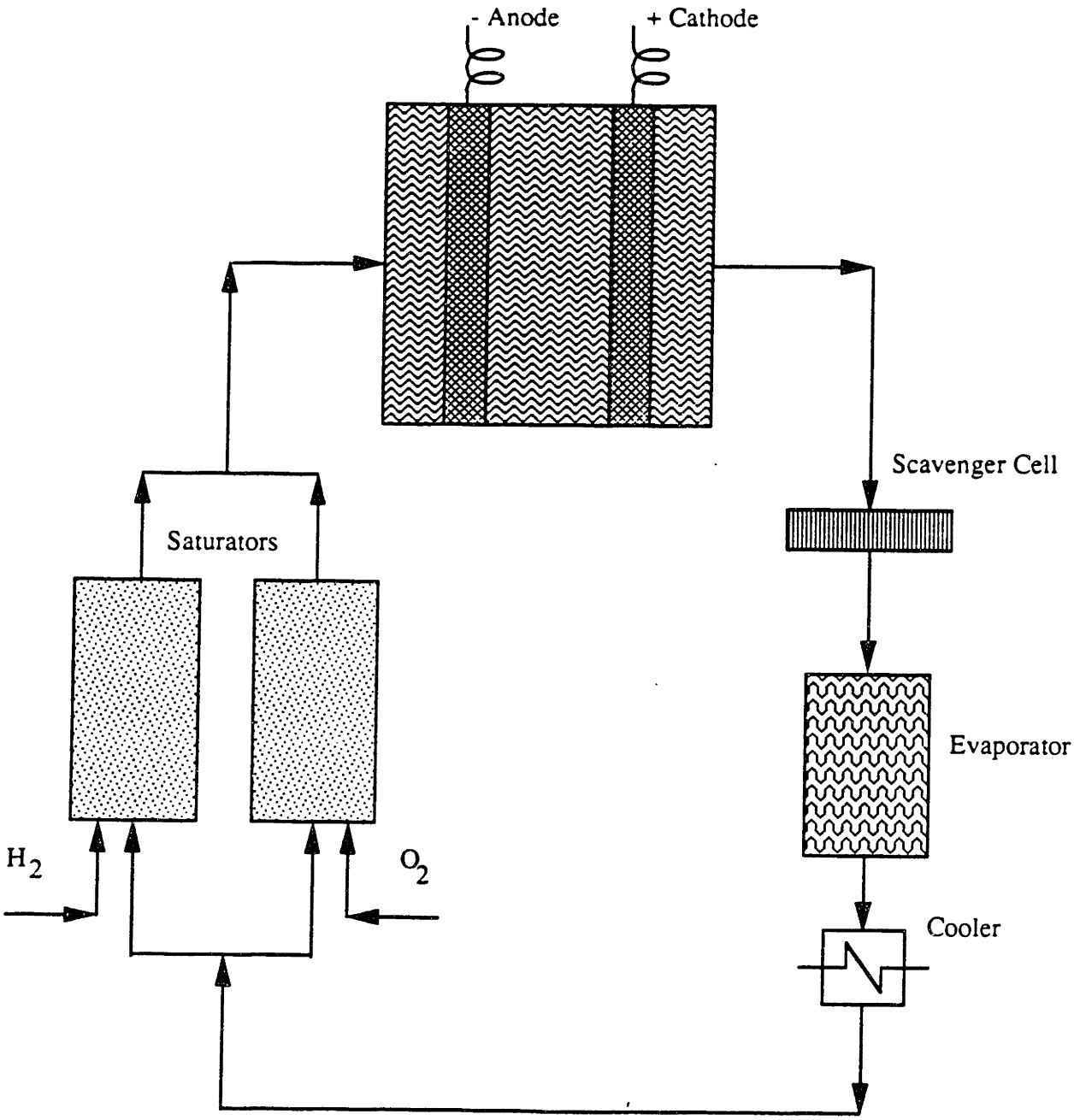

Source: Holeschovsky, 1991 [29]

Figure 1-5: Schematic diagram of a mixed feed flooded flow fuel cell system

Once again the rate of electrochemical reaction can be controlled to some extent by varying the flow rate of the gas-electrolyte mixtures. However, the gases in the mixed feed system must be supplied in a stoichiometric 2 to 1 ratio, and the system is restricted to a single electrolyte.

Several mutual advantages are anticipated from these configurations. The effective surface area will be increased; therefore, the practical current density levels should increase. Less sophisticated electrodes will be required because no pure gas phases will be present. Also, the lack of gas phases should yield a more rugged design which is more resistant to shocks and vibrations. Temperature control should also be considerably easier. Since gas compartments will no longer be needed within the stacks, the volume occupied by the fuel cell stacks should decrease. The result of these advantages should yield both a lower cost and a better power output per unit weight and volume than is found in conventional fuel cells.

1.6.2 Importance of Hydrogen and Oxygen Solubility

Gas solubilities are particularly important for flooded flow fuel cells because the amount of fuel and oxidant supplied to the electrodes is proportional to the solubility of hydrogen and oxygen in the electrolyte solution(s). Gas solubilities are one of three factors which may limit current densities in flooded flow fuel cells. The other two limiting factors are the electrochemical reactions and mass transfer. The solubility is important because it represents the maximum amount of fuel and oxidant available for reaction, which in turn has a significant influence on the mass transfer of the gases.

It appears that the most significant limiting factor on the theoretical current obtainable from a flooded flow fuel cell is the mass transfer of the oxygen and the nydrogen to the surface of the electrodes. However, although beyond the scope of this thesis, it may be possible to sufficiently increase the value of the mass transport such that it is no longer a limiting factor. In this case, the maximum performance is controlled by solubility limitations. The solubility does not influence the kinetics of the electrochemical reaction. For simplicity and to focus on the effects of solubility,

it is assumed here that reaction kinetics are not limiting.

Flooded flow fuel cells of a given electrolyte type will need to be able to support at least the same current density as their conventional counterparts in order to be competitive. Since both the solubility and mass transfer limitations can be reduced by increasing the flow velocity, these factors should theoretically be reducable to negligible levels by sufficiently increasing the electrolyte flow velocity. However, the parasitic power losses due to pumping requirements and the structural limitations of the fuel cell need to be carefully considered. It has been estimated that flow velocities of approximately 10 cm/s would be acceptable; however, this rate is only a rough approximation which was proposed by Holeschovsky [29]. The maximum acceptable velocity is more likely 2-5 times higher than this. Should flooded flow fuel cells require still higher electrolyte flow velocities, their feasibility is questionable.

Chapter 2

Objectives and Approach

This investigation first explores the basic theory underlying the solubility of gases in liquids. Concepts such as fugacities, activity coefficients, and salting coefficients are presented in a thermodynamic context. The effects of pressure and temperature on solubility are presented briefly from a theoretical standpoint. While no general relationships can be established for all electrolytes, Henry's law can be assumed to hold for all of the aqueous electrolytes presented here because water obeys Henry's law at the pressures at which fuel cells are operated. Molten carbonate electrolytes, however, have been observed to not obey Henry's law.

Several techniques have been used to measure solubilities. The most frequently used techniques are presented along with a brief assessment of their reliability in terms of both accuracy and precision. Since researchers present the solubility data in terms of a number of different parameters, the various solubility parameters are defined, along with the formulae used to interrelate parameters in this study.

The Ostwald coefficient was chosen in this investigation as the means of presenting comparisons of the solubility of hydrogen and oxygen in electrolytes. This is a parameter which can be easily manipulated and converted to other terms. In order to derive the Ostwald coefficient from salting coefficient data, values for the solubility of hydrogen and oxygen in water must be available. The solubilities in water were drawn from equations which best fit the data obtained by a number of researchers, and presented in a tabular and a graphical fashion. These values are believed to be

quite accurate.

The salting coefficients for hydrogen and oxygen in electrolytes pertinent to flooded flow fuel cell applications are presented in tabular form as a function of temperature (and concentration for sulfuric acid) along with footnotes indicating the source of the data. Much of the data was drawn from two volumes of the *Solubility Data Series* [7, 59]. The remainder of the data was drawn from a variety of investigations and converted to a common set of units. Summaries of these studies and the procedures by which the data was converted to salting coefficients are presented in an Appendix A.

Solubilities, in terms of the Ostwald coefficient, were computed and presented graphically as a function of temperature and electrolyte concentration. Factors which limit performance were then computed for each flooded flow electroyte system at representative operating conditions. For studies which presented diffusivity data as well as solubility data, the mass transfer limit was computed, assuming all reactants are consumed. Minimum electrolyte velocities were determined for these limits. Since flooded flow fuel cells would need to perform at least as well as conventional fuel cells, the solubility and mass transfer limited performance levels were then compared to the performance of conventional fuel cells. Based upon the magnitude of the required flow rates, the feasibility of the flooded flow fuel cell system was assessed for the various electrolytes.

Chapter 3

Solubility Measurements

Solubilities, though studied for more than a century, are still largely an unresolved area of chemical science. Some systems, such as the solubility of oxygen in water at atmospheric conditions, are very well researched and are believed to have very accurate solubility assessments. However, most systems (if studied at all), have been given rather uncertain assessments. Theoretical predictions are even more difficult to make than experimental evaluations.

3.1 Theoretical Considerations

Gas molecules dissolve in a liquid when they move into the surface of the liquid with sufficient energy to enter the liquid. However, a solute molecule, in general, does not have enough energy to "dig its own hole." Instead, gas molecules enter through naturally occuring microscopic "cavities" in the surface of the solvent. Thus, the solubility of a liquid will be a function of both the energy of the gas molecule and the number and nature of the "cavities" in the surface of the liquid [41].

While it may appear that the nature of the cavities may be related to some measurable property, such as surface tension, this is not actually the case. Battino and Young have suggested that macroscopic properties such as surface tension are inadequate measures of the microscopic properties upon which solubilities are based. They claim, "The criticism that the bulk surface tension is not appropriate to calculate the

energy of formation of a molecular-sized cavity seems justified. Rather the surface tension is probably proportional to some solvent property that determines the gas dissolving power of the solvent" [8]. This does not, however, mean that investigators are without tools for determining solubilities. It just means that it is a complicated phenomenon which can not be addressed by simply correlating the solubility to some readily observable and/or tabulated macroscopic properties.

3.1.1 Thermodynamics of Fluid-Phase Equilibria

Solubility can be analyzed as a fluid-phase equilibrium problem such as has been described by Prausnitz [42]. This class of problems is solved by introducing the abstract concept of the *chemical potential* of the system to determine the thermodynamic solution. The chemical potential is expressed in terms of change in chemical potential caused by a change in the intensive quantities of temperature, pressure, and/or the partial molar Gibbs energy. Since there is no immediate equivalent to chemical potential in the real world, a correlation term, *fugacity*, is introduced to help determine the chemical potential. The fugacity, f, is a convenient function which facilitates the transition from the "ideal" world of pure thermodynamics to the theory of intermolecular forces which allows for corrections to the thermodynamic solution caused by "non-ideality."

The activity coefficient of a system indicates how "active" a substance is relative to a standard state. The activity is defined as

$$a \equiv \frac{f}{f^o}, \tag{3.1}$$

where f^o is the fugacity at some specified condition known as the standard state. For the analysis of the solubility of gases in liquids, the standard state which is generally used is the fugacity of an infinitely-dilute solute gas in water at the same temperature and pressure.

For any species i at equilibrium, the fugacities must be the same in all phases.

For two phases, α and β,

$$f_i^\alpha = f_i^\beta. \tag{3.2}$$

This relationship forms the basis of solubility analyses based upon the thermodynamics of fluid-phase equilibrium.

3.1.2 Other Theoretical Approaches

Regular solution theory has been developed and utilized by Hildebrand and Scott [28] to explain solubility phenomena. They define a regular solution as a solution involving no entropy change when a small amount of one of its components is transferred to it from an ideal solution of the same composition, with the total volume remaining unchanged.

Computer simulations have been successfully applied to predict the solubility of gases in water. These can be utilized for any solute-solvent system provided the complicated geometry and interaction potentials can be successfully modeled. Although computer methods have potential, they are as of yet, not terribly accurate for most systems.

3.1.3 Salt Effects

The cause of the difference in activity between a system with a pure solvent and one with a solution consisting of that solvent and a salt is referred to as the *salt effect.* The salt effect can be used to describe the solubility of a gas in an aqueous salt solution relative to the solubility of that gas in pure water. An excellent discussion of salt effects has presented by Battino and Young [8, p. 416-419]. They selected the salting coefficient as the most convenient method of comparing solubility data in the solubility data compilations that they prepared [7, 59].

The salt effects can be derived using the molecular thermodynamics of fluid-phase equilibrium. The activity coefficient can be represented by a power series in C_s, the electrolyte concentration, and C_i, the nonelectrolyte solute gas concentration, as

follows

$$log f_i = \sum_{mn=0} k_{mn} C_s^n C_i^m. \tag{3.3}$$

For low C_s and C_i where there is no chemical interaction between solute species, the nonlinear terms can be dropped, yielding

$$log f_i = k_s C_s + k_i C_i. \tag{3.4}$$

Furthermore, for the solubilities considered here, C_i is quite small and allows the latter term to be ignored. Thus, this can be simplified to

$$log f_i = k_s C_s. \tag{3.5}$$

It is also known that, for a given partial pressure of the solute gas, the activity is the same in the pure solvent and the salt solution. (Note that water is the pure solvent for aqueous electrolytes.) Therefore,

$$f_i S_i = f_i^o S_i^o, \tag{3.6}$$

where S_i and S_i^o represent the gas solubility in salt solution and water. Equation 3.6 can be rearranged and combined with equation 3.5 to obtain

$$log f_i = log f_i^o + log \frac{S_i^o}{S_i} = k_s C_s + k_i S_i. \tag{3.7}$$

Since $log f_i^o = k_i^o S_i^o$,

$$log \frac{f_i}{f_i^o} = log \frac{S_i}{S_i^o} = k_s C_s + k_i (S_i - S_i^o). \tag{3.8}$$

Assuming that $S_i \approx S_i^o$, the following equation results

$$log \frac{S_i^o}{S_i} = k_s C_s. \tag{3.9}$$

Equation 3.9 is in the same form as the Setschenow equation for the solubility

of electrolyte solutions, $log S_i^o/S_i = KC_s$. However, if the assumption that $S_i \approx S_i^o$ does not hold, K and k_s will not be the same. This distinction is important when comparing the salt effects of a non-electrolytes of low solubility with one of high solubility. This will not be an issue with the systems considered here.

Thus, the salting coefficient represents the impact of salt concentration on the activity coefficient of a solution for a given gas. A salt which increases the activity coefficient of a dissolved gas is said to salt-out that gas, while conversely, a salt which decreases the activity coefficient is said to salt-in. In other words, a positive salting coefficient, which indicates that a gas is less soluble in a salt solution than it is in water, indicates that the gas is salted out; a negative salting coefficient indicates that the gas is salted in and is more soluble in the salt solution than in water. Some salt solutions are known to salt in at certain concentrations and temperatures, but salt out at others.

3.1.4 Influence of Temperature and Pressure

While there is a marked paucity of data for the solubility of hydrogen and oxygen in electrolytes at high pressures, Henry's Law is assumed to generally apply to aqueous electrolyte solutions within the pressure ranges where it is obeyed for pure water solubility. Henry's Law states that at constant temperature, the fugacity of the gas solute is proportional to the mole fraction of that solute, in the liquid. The constant of proportionality, the Henry's law coefficient, depends upon temperature, and to a lesser degree, pressure. At the low pressures of interest in this study, however, the pressure effects for water are negligible.

It is often correct to assume that as temperature rises, gas solubility falls. However, this is not always the case. Furthermore, Prausnitz et. al [42, p. 382] concluded, "No simple generalizations can be made concerning the effect of temperature on solubility..." In a few specific cases, the mole fraction solubility dependence on temperatures

can be represented by an equation of the form

$$lnx = A + \frac{B}{(T/100K)} + Cln(T/100K) + D(T/100K). \tag{3.10}$$

Equations of this type are derived for specific systems and conditions; thus, the coefficients A, B, C, and D are not generally applicable.

3.2 Experimental Techniques

Many different techniques have been employed to measure the solubility of gases in liquids. These techniques vary markedly in cost, complexity, time requirements, and precision. Many factors contribute to variations among reported solubility measurements. The easiest to regulate are the purity of materials, pressure, volume, and temperature. According to Cook [17], "temperature control of $\pm 0.1°$ should be more than adequate for most purposes" [8, p. 399]. The large discrepancies which often appear in the literature are usually due to other factors. Cook and Hanson [18] have identified these as being one or more of the following: (a) failure to attain equilibrium; (b) failure to completely degas the solvent; (c) failure to ascertain the true amount of gas dissolved; and (d) failure to make certain that the transfer of gas from a primary container to the apparatus does not involve contamination [19].

3.2.1 Manometric-Volumetric Methods

Manometric and volumetric methods involve the careful measurement of the temperature, volume, and pressure of both the solute gas and the solution. The solute gas is then bubbled through the solution at constant temperature and pressure until steady state is reached. The new partial pressure of the solute gas above the solution is measured at steady state. Since the volume of gas that dissolves in the solution is negligible compared to the volume of the solution, the volume that the undissolved gas will occupy above the liquid will be the same as it was at the start. By measuring the pressure of the gas above the solution, the amount of gas remaining undissolved

in the solution can be determined. The solubility of the gas will then be the difference of the original quantity of gas from the remaining quantity of gas, divided by the quantity of solution. As will be seen in the next section, these quantities can be moles, masses, or volumes, according to the preference of the researcher.

The accuracy and precision obtained is heavily dependent upon the specific apparatus used and the care taken by the researchers. The best precision obtained for this class of measurements was obtained by Cook and Hanson, who reported results which were accurate and reproducable to $\pm 0.1\%$ [19]. While the applicability of manometric and volumetric methods are dependent upon the apparatus and the care of the researchers, as a general rule, they are not well suited for measuring mole fraction solubilities as low as 10^{-5} - 10^{-8}.

A related solubility measurement technique involves saturation methods. The saturation method of measuring the solubility of a gas dissolved in a liquid attains saturation by flowing a liquid film through a gas instead of bubbling the gas through the liquid. Many different apparatuses have been developed for experimentally using this concept [8].

3.2.2 Mass Spectrometric Methods

This technique involves the "outgassing" of a sample of a gas-saturated solvent, trapping the gas, and then analyzing the gas by mass spectrometry to determine the solubility of the gas in the solvent. According to Battino, a prime advantage of the mass spectrometric method is the ability to determine the ratio of dissolved gases and isotope effects in dissolved gases. Additionally, this technique has the flexibility to determine the solubility of a pair of solute gases by simply using standard values for the solubility of one of the gases [8]. Hence, this technique may be ideally suited for determining the solubility of hydrogen and oxygen in the electrolyte of a mixed feed flooded flow fuel cell.

3.2.3 Gas Chromotographic Methods

This dynamic technique is important for measuring solubilities too low to be measured by the standard static techniques. It involves injecting the gas-saturated liquid solution in a column where it is usually vaporized and mixed with a carrier gas (eg. helium). The column frequently contains an inert stationary liquid support phase. The feed is continually bathed by a carrier gas which reaches an equilibrium point at which a constant volume of gas is dissolved into the stationary liquid support. A third substance (vapor, gas, or a mixture) is then used to partition the carrier gas stream off from the stationary liquid. By knowing the retention volumes, column characteristics and dimensions, and the quantity of partitioning liquid, it is possible to determine gas solubilities. Gas solubilities measured in this way are measured for systems under special constraints. Battino [8, p. 403] identified these constraints as follows:

- The liquids are restricted to high boilers.
- The solubility is for a gas or vapor in a film of liquid (supported on a solid phase) and in which the carrier gas is already equilibrated.
- The process involves steady states and transient equilibriums as the carried component is swept through the column.
- In the portion of the gas stream where the carried component is, the carrier gas concentration is less than normal and as this portion of the gas stream passes any given point some of the carrier gas must be outgassed.
- It is difficult to ascertain the carried component partial pressure as it is swept along as a band which may or may not be symmetrical in its concentration distribution.

Gas chromatography in gas solubility determinations has been primarily used as an analytical tool for the quantification of gases extracted from saturated solutions of liquids. While gas chromatographic methods are similar to the mass spectrometric

methods described in the last section in this sense, gas chromatography offers several advantages over mass spectrometry. Gas chromatography is relative simple, cheap, and facilitates rapid solubility measurements. The reproducibility of a gas chromatographic analysis is of the order of 1-2%, but uncertainties in the extraction of the dissolved gas typically makes the over-all precision 3% or less [9, 8].

3.2.4 Chemical Methods for Dissolved Oxygen

The Winkler method [57], and its modifications, are the most accurate of the chemical methods [8]. Other chemical methods, including the Van Slyke technique [55], are occasionally used for solubility measurements, but the Winkler method appears to be the most popular.

The Winkler method involves the oxidation of freshly precipitated manganous hydroxide by the dissolved oxygen to form manganic hydroxide in a high pH environment. The solution is then made acidic causing the the manganic ion to oxidize iodide. In the presence of excess iodide, the iodine is largely present as the complex triodide. Lastly, the iodine is titrated with thiosulfate which is oxidized to tetrathionate. The excess thiosulfate is back-titrated amperometrically with standard potassium iodate reagent. The equations for these steps are as follows:

$$Mn^{2+} + 2OH^- = Mn(OH)_2 \tag{3.11}$$

$$2Mn(OH)_2 + \frac{1}{2}O_2 + H_2O = 2Mn(OH)_3 \tag{3.12}$$

$$2Mn(OH)_3 + 6H^+ + 3I- = 2Mn^{2+} + I_3^- + 6H_2O \tag{3.13}$$

$$I_2 + I^- = I_3^- \tag{3.14}$$

$$I_2 + 2S_2O_3^{2-} = 2I^- + S_4O_6^{2-} \tag{3.15}$$

The Winkler method depends on strict control of pH and iodide concentration [8, p. 404].

The error associated with the Winkler method was a subject of much work during

the 1960s. According to Dr. B.A. Southgate, the Director of Water Pollution Research at the Water Pollution Research Laboratory, Stevenage, Herts., England: "One thing which has come out of this work [38] is that it is pretty obvious that a very large proportion of the determinations of dissolved oxygen made before about 1961 or 1962 must have been incorrect for the same reason that the solubility values determined by Truesdale [54] were incorrect. The biggest source of possible error of course occurs if one uses the present-day accurate values for solubility with incorrect determinations of concentration in water, and from these two values calculates the oxygen deficit" [8, p. 405]. Hence, those investigations cited in this report that were carried out prior to 1961 must be regarded as somewhat uncertain.

More recently, this problem has been largely solved. Battino noted that the agreement among recent workers is excellent, and it appears that a truly definitive set of values for the solubility of oxygen in pure water has been attained" [8, p. 406]. These data are presented in Table 3.1 on page 55 in section 3.4.1. It is very important because the solubility of gases in pure water is the standard against which the salting coefficient for aqueous salt solutions are derived.

3.3 Methods of Expressing Solubility

Since the representations of solubility are numerous, it is important to clearly specify the method used. Furthermore, relative solubilities represented by one method may not correspond to those of another. For example, "in the third edition of Hildebrand and Scott's *Solubility of Nonelectrolytes* [28] they present a table showing the solubility of sulfur (S_8) at 25°C in benzene and toluene. In weight per cent sulfur is more soluble in benzene; however, in mol per cent or grams per liter sulfur is more soluble in toluene" [7, p. xi].

This problem can also be observed in the data presented in this study. For example, the solubility of hydrogen in terms of mol fraction appears higher at T = 288.15K (x_1 = 1.510) than the solubility at T = 353.15K (x_1 = 1.371), while conversely, the solubility of hydrogen in terms of the Ostwald Coefficient appears lower

at $T = 288.15$K ($L = 1.980$) than the solubility at $T = 353.15$K ($L = 2.144$). This is associated with the slightly different shapes of the curves shown in Figures 3-1 and 3-2. The different shape of the solubilty curves, in terms of the Ostwald coefficient and the mol fraction, is related to the change in density as a function of temperature.

Solubility is generally represented as a measure of the "amount" of solute gas to be absorbed in a given "amount" of solution. The following are some of the most popular methods of expressing solubility.

3.3.1 The Bunsen Coefficient, α

The Bunsen coefficient is a dimensionless parameter which is defined as the volume of gas, reduced to a temperature of 0°C and a pressure of 1 atm, which is absorbed by a unit volume of solvent (at the temperature of the measurement) under a gas pressure of 1 atm. When the partial pressure of the gas above the solvent deviates from 1 atm, Henry's Law can be used to compute a Bunsen coefficient which is corrected for pressure. (Note that this assumes that the pressure is within certain limits. The pressures found in the fuel cell environment should fall within these limits.) The Bunsen coefficient is expressed as

$$\alpha = \frac{V_g}{V_s}\frac{273.15}{T}, \tag{3.16}$$

where V_g is the volume of the gas absorbed, V_s is the volume of the absorbing solvent, and T is the absolute temperature of the system. Consequently, the Bunsen coefficient, when converted from total pressures to the partial pressure of the gas, is frequently referred to as the absorption coefficient or the coefficient of absorption [8, 7].

3.3.2 The Absorption Coefficient, β

At a total pressure of 1 atm and a temperature of 273.15K, the absorption coefficient is expressed as

$$\beta = \alpha[1 - P(l)], \tag{3.17}$$

where $P(l)$ is the partial pressure of the liquid in the atmosphere. The frequently cited units of β are atm [8, 7].

3.3.3 The Ostwald Coefficient, L

The Ostwald Coefficient is a dimensionless parameter which is defined as

$$L = \frac{V_g}{V_s}, \tag{3.18}$$

where V_g and V_s are measured at the same temperature. The Ostwald Coefficient can also be expressed in terms of gas concentrations by

$$L = \frac{C_l}{C_g}, \tag{3.19}$$

where C_l is the concentration of the gas in the liquid phase and C_g is the concentration of the gas in the gas phase. The Ostwald coefficient is an equilibrium constant. Thus, assuming the gas can be modeled as an ideal gas, it is then independent of the partial pressure of the gas, and only depends on temperature for a given system. However, when fixing the value of the Ostwald coefficient, one must designate a constant temperature and total pressure.

If the total pressure is kept at 1 atm, then the volume of gas absorbed, reduced to 0°C and 1 atm by the ideal gas laws, per unit volume of liquid is equal to the absorption coefficient, β. It is important to clearly specify the method of calculating the solubility since β sometimes gets confused with α. [8, 7].

3.3.4 The Weight Solubility, C_w

The weight solubility is defined as the number of moles of dissolved solute gas, at a partial pressure of 1 atm, per gram of solvent. The units of C_w are mol/g [8, 7].

3.3.5 The Kuenen Coefficient, S

The Kuenen coefficient is defined as the volume of gas (in cubic centimeters) at a partial pressure of 1 atm reduced to 0°C and 1 atm, dissolved by the quantity of solution which contains 1 g of solvent. Thus, S is proportional to the gas molality [8, 7].

3.3.6 The Henry's Law Constant

For a gas in equilibrium with a liquid, Henry's Law is denoted by

$$P_g = K_1 x_g, \tag{3.20}$$

where x_g is the mole fraction solubility, P_g is the partial pressure of the gas, and K_1 is a constant. Solubilities may be expressed in terms of mole fractions, as well as volume fractions, molarity, and molality. In the case of a dilute solution, Henry's Law can be presented as

$$P_g = K_2 C_l \tag{3.21}$$

and

$$C_g = K_c C_l, \tag{3.22}$$

where C_l and C_g are the concentrations of the liquid and the gas phase.

From the last equation, it is apparent that $K_c = 1/L$. The Henry's Law constants (K_1, K_2, and K_c) can all be used to represent solubility, where K_1 is in units of atm, K_2 is in $atm\text{-}l/mol$, and K_c is dimensionless. However, it must be remembered from thermodynamics that Henry's Law is applicable only over a restricted pressure range for dilute solutions and is actually just a limiting law. To avoid ambiguity, the method of calculating the Henry's Law constant must be specified, [8, 7]. According to Battino, "The practice of converting solubility data from the experimental pressure to a partial gas pressure of 1 atm by applying Henry's Law usually introduces no errors if the pressure range is reasonably small" [8, p. 407]. For the solubility of hydrogen and oxygen in water, "reasonably small" implies pressures of less than 50 to 100 bars

[52, 56].

3.3.7 The Mole Fraction, x_g

For a binary system, the liquid phase mole fraction of solute absorbed (the solubility) is a dimensionless parameter given by

$$x_g = \frac{n_g}{n_g + n_l} = \frac{W_g/M_g}{[W_g/M_g] + [W_l/M_l],} \tag{3.23}$$

where n_i is the number of moles, W_i is the mass, and M_i is the molecular weight of the solute gas (for $i = g$) or the liquid solvent (for $i = l$). The partial pressure of the gas and the measurement temperature should be specified to avoid ambiguity [7].

3.3.8 The Weight Per Cent Solubility, $wt\%$

For a binary system, the weight per cent is a dimensionless parameter defined as

$$wt\% = 100\frac{W_g}{W_g + W_l}, \tag{3.24}$$

where W is the weight of the gas or liquid [7].

3.3.9 The Moles Per Unit Volume Solubility, n or c_g

When the density of the liquid component is not known for a given system, the solubility may be represented in terms of moles of gas per unit volume of the liquid mixture. The units of this solubility expression are typically given as mol/l or mol/cm^3 [7].

This solubility measure is related to the mole fraction solubility by

$$n = MW_l \rho_l x_g, \tag{3.25}$$

where MW_l and ρ_l are the molecular weight and the density of the liquid mixture, and x_g is the mole fraction of solute absorbed. This measure is especially useful for expressing solubilities when the density of the liquid mixture is not known.

3.3.10 The Mole Ratio, N

The mole ratio is a dimensionless parameter which is defined as

$$N = n_g/n_l, \tag{3.26}$$

where n is the number of moles of gas or liquid [7].

3.3.11 The Salting Coefficient, k_{sc_α}

The equations relating the influence of salting on activity coefficients to the influence on solubility are as follows:

$$k_{sc_\alpha} = \frac{log(\alpha^\circ/\alpha)}{c_2}, \tag{3.27}$$

$$k_{sc_L} = \frac{log(L^\circ/L)}{c_2}, \tag{3.28}$$

$$k_{sc_c} = \frac{log(c^\circ_{1,sat}/c_{1,sat})}{c_2}, \tag{3.29}$$

where α is the Bunsen coefficient, L is the Ostwald coefficient, c_1 is the molar gas solubility, c_2 is the electrolyte concentration in mol/l, and the superscript ($^\circ$) refers to the pure solvent (water, for all systems considered in this work). The units of these three salting coefficients are l/mol.

Since

$$\alpha^\circ/\alpha = L^\circ/L = c^\circ_{1,sat}/c_{1,sat}, \tag{3.30}$$

it follows that

$$k_{sc_\alpha} = k_{sc_L} = k_{sc_c}. \tag{3.31}$$

Thus, these salting coefficients can be used interchangeably.

Some other forms of the salting coefficient which may be relevant to solubility studies are:

$$k_{sm_s} = \frac{log(S^\circ/S)}{m_2}, \tag{3.32}$$

$$k_{sc_x} = \frac{log(x^\circ/x)}{c_2}, \tag{3.33}$$

$$k_{sm_x} = \frac{log(x^\circ/\mathrm{x})}{\mathrm{m_2}}, \tag{3.34}$$

where m_2 is the electrolyte molality, S is the Kuenen coefficient, and x is the mole fraction solubility. k_{sm_s} and k_{sm_x} are in units of $l/g\text{-}mol$; k_{sc_x} is in units of l/mol.

The salting coefficient reflects the decrease in solubility associated with the increase in concentration of a salt in water. Thus, the solubility of a gas in water represents an upper bound on the solubility of the gas in an aqueous salt solution. Note that the larger the salting coefficient, the lower the solubility for a given gas and salt solution [8, 7].

3.4 Solubility of Hydrogen and Oxygen in Water

The salt effect indicates that for a given temperature, the solubility of salt solution is equal to the solubility of the gas in water times a constant of proportionality which is a function of salt concentration. As a result, the shape of the solubility vs. temperature curves for gases in low concentraton salt solutions are often similar to those for the solubility of the same gases in pure water. At higher concentrations, however, solubility-temperature behavior can be quite different than the behavior for pure water.

3.4.1 Solubilties at Pressures up to 200 kPa

The solubility of oxygen in water at atmospheric pressure has been one of the most intensively studied gas solubility systems [7, p. 1]. The correspondence between the values for the solubility of oxygen in water obtained by the various methods described above is quite good. The best curve fit to the experimental data for the solubility of oxygen in water is given by Battino [7] as

$$lnx_1 = -66.73538 + \frac{87.47547}{T/100K} + 24.45264ln(T/100K), \tag{3.35}$$

T (K)	HYDROGEN Mol Fraction x_g x 10^5	HYDROGEN Ostwald Coefficient L x 10^2	OXYGEN Mol Fraction x_g x 10^5	OXYGEN Ostwald Coefficient L x 10^2
273.15	1.755	2.184	3.949	4.913
278.15	1.657	2.100	3.460	4.384
283.15	1.576	2.032	3.070	3.958
288.15	1.510	1.980	2.756	3.614
293.15	1.455	1.940	2.501	3.333
298.15	1.411	1.911	2.293	3.104
303.15	1.377	1.893	2.122	2.918
308.15	1.350	1.883	1.982	2.766
313.15	1.330	1.883	1.867	2.643
318.15	1.317	1.890	1.773	2.545
323.15	1.310	1.905	1.697	2.468
328.15	1.308	1.927	1.635	2.409
333.15	1.312	1.957	1.586	2.367
338.15	1.320	1.993	1.549	2.339
343.15	1.333	2.037	1.521	2.325
348.15	1.350	2.087	1.502	2.323
353.15	1.371	2.144		

Sources: Battino [7] and Young [59]
Note: Data point for $L(H_2)$ at T = 278.15K was listed as 2.010 in the literature. This appears to have been a typographical error as 2.100 appears to be a more appropriate value.

Table 3.1: Smoothed Data for the Solubility of Hydrogen and Oxygen in Water for Low Temperatures at a Partial Pressure of 1 atm

where x_1 is the mole fraction solubility at 1 atm partial pressure of gas. Battino has recommended this equation for temperatures between 273 and 373K. Data tabulated by Battino in terms of mole fractions and the Ostwald coefficient are shown in Table 3.1. Note that the mole fractio solubilities shown in Figure 3-1 make up a slightly different shaped curve than those for the Ostwald coefficient solubilities shown in Figure 3-2. For temperatures greater than 373K, Battino took high pressure data and presented it as mole fractions at atmospheric pressure. These data, along with the corresponding Ostwald coefficients appear in Table 3.2.

Young [59] has presented an equation which represents the best fit to experimental

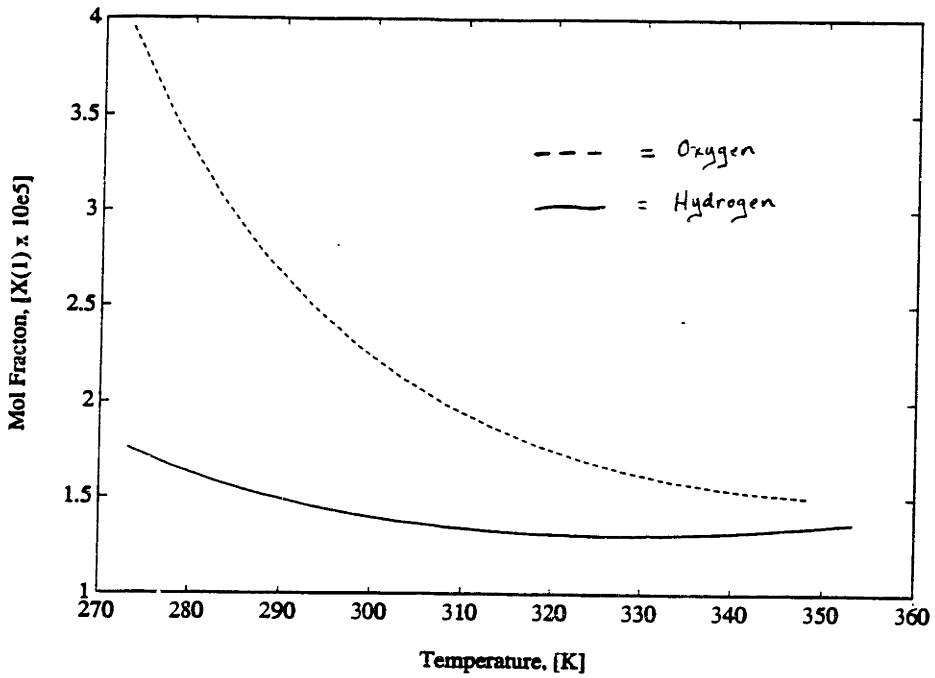

Sources: Battino [7] and Young [59]

Figure 3-1: Mole Fraction Solubility of Hydrogen and Oxygen in Water at Low Temperatures and a Partial Pressure of 1 atm

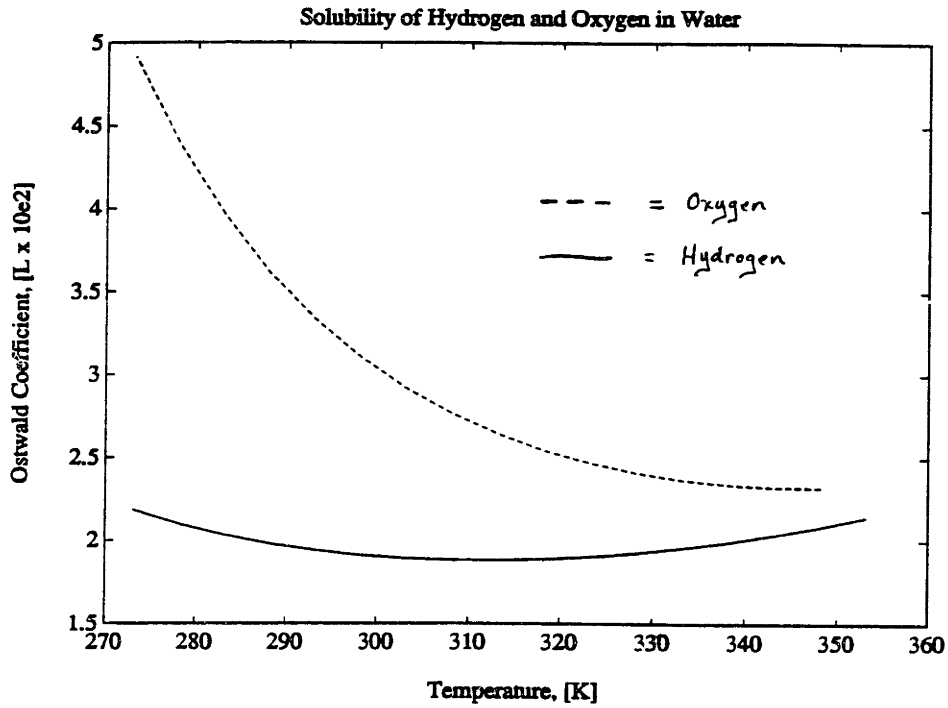

Sources: Battino [7] and Young [59]

Figure 3-2: Ostwald Coefficient Solubility of Hydrogen and Oxygen in Water at Low Temperatures and a Partial Pressure of 1 atm

T (K)	HYDROGEN Mol Fraction x_g x 10^5	HYDROGEN Ostwald Coefficient L x 10^2	OXYGEN Mol Fraction x_g x 10^5	OXYGEN Ostwald Coefficient L x 10^2
353	1.37	2.25	1.44	2.14
363	1.43	2.25	1.41	2.28
368	1.46	2.26	1.40	2.36
373	1.50	2.30	1.41	2.45
378	1.55	2.34	1.42	2.55
383	1.60	2.39	1.44	2.65
388	1.65	2.44	1.46	2.77
393	1.71	2.50	1.48	2.89
398	1.77	2.57	1.51	3.03
403	1.84	2.65	1.54	3.18
408	1.92	2.74	1.57	3.34
413	2.00	2.83	1.61	3.51
418	2.09	2.94	1.66	3.70
423	2.18	3.05	1.71	3.90
473	3.62	4.83	2.51	6.98
523	6.46	8.29	4.04	13.28

Sources: Battino [7] and Young [59]

Table 3.2: Selected Values from the Smoothed Data for the Solubility of Hydrogen and Oxygen in Water for High Temperatures at a Partial Pressure of 1 atm

data for the solubility of hydrogen in water:

$$ln\ x_1 = -48.1611 + \frac{55.2845}{(T/100K)} + 16.8893\ ln\ (T/100K). \qquad (3.36)$$

Young presented tabulations of the mole fraction solubility and the Ostwald coefficient for temperatures ranging from 273.15 to 353.15K. Since he did not specify a limited temperature range over which this equation is valid, it was used to determine solubilities at higher temperatures as well. These data are shown in Table 3.1 and Table 3.2.

The values which appear in both of these tables are combined in Figure ??. It is interesting to note that the low temperature curve for oxygen appears to flow smoothly into the high temperature curve for hydrogen. Likewise, it appears that the low temperature curve for hydrogen appears to continue along into the high temperature curve for oxygen. Provided that the information was provided correctly by Battino and Young, this is just a conicidence, and there is a slight discontinuity in each of the curves.

It should also be noted that in deriving Ostwald coefficient solubility values for hydrogen and oxygen in water at high temperatures, I approximated the density of water as a linear extension of data found for temperatures between 340 and 373K. The equation used for this extrapolation was

$$\rho_{H_2O} = 1.19974 - (6.646x10^{-4})\ T. \qquad (3.37)$$

In comparing the densities obtained from this correlation to those presented in a standard set of steam tables, it can be seen that between 373K and 423K, the error introduced by this approximation is less than 1%. At a temperature of 523K, there is an error of approximately 6.6% introduced, and at a temperature of 473K, the error is approximately 2.4%. Thus, over the temperature range of interest for this investigation, equation 3.37 is adequate. A comparison of the data is presented in Figure 3-4. For a more rigorous calculation, direct access to a computer-based form of the steam tables or a linear interpolation of the steam table data presented in Table ??

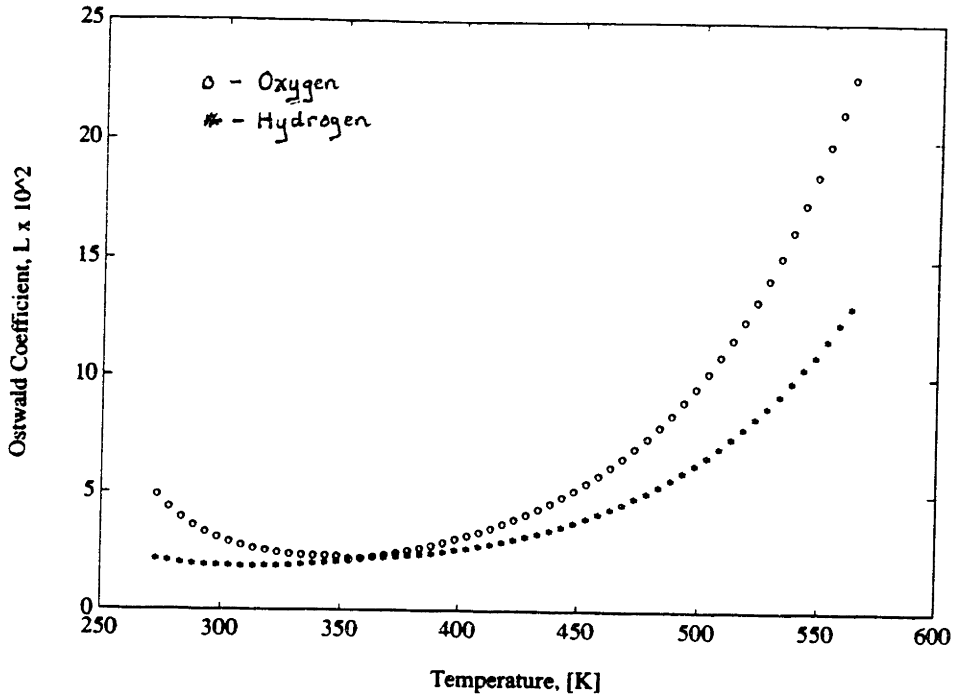

Sources: Battino [7] and Young [59]

Figure 3-3: Ostwald Coefficient Solubility of Hydrogen and Oxygen in Water at a Partial Pressure of 1 atm Over a Broad Range of Temperatures

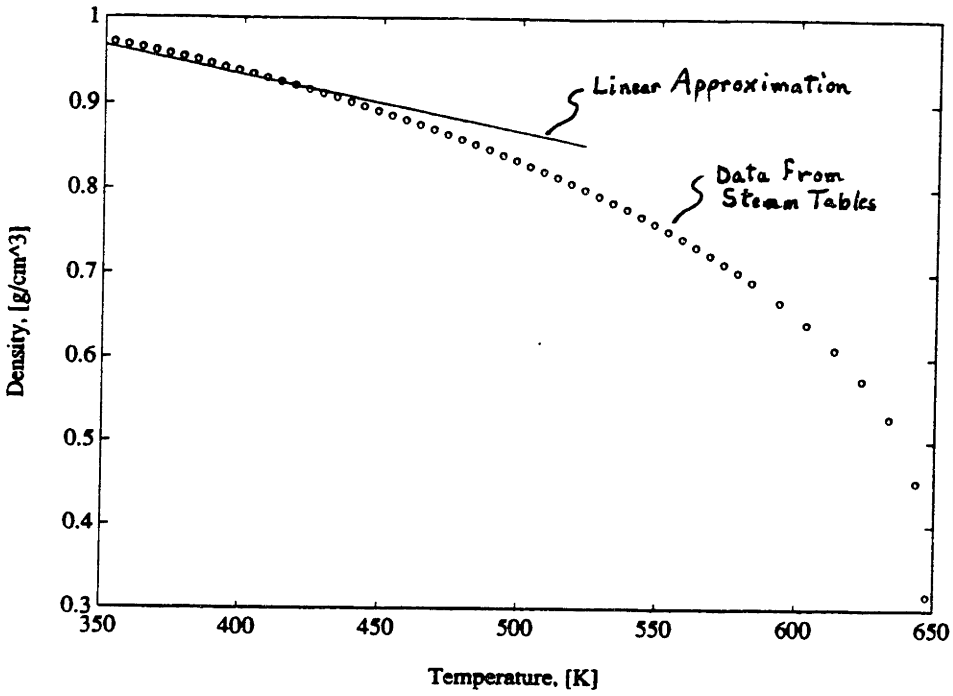

Figure 3-4: Comparison of the Temperature-Correlated Approximation of the Density of Water to the Densities Tabulated in the Steam Tables

could be used. However, for the purposes of this investigation, the correlation given by equation 3.37 should be sufficiently accurate, especially since solubility values presented for electrolytes are not that accurate themselves. The only study which would incur noticeable errors (greater than 1%) with the correlation approximation is the that of Bruhn, Gerlach, and Pawlek [14] who measured solubilities at temperatures as high as 473 and 523K. The remainder of the solubility measurements were for temperatures of no more than 423K, where the error is less than 1%.

Temp. (K)	Density (g/cm^3)	Temp. (K)	Density (g/cm^3)
353.15	0.9717	483.15	0.8528
358.15	0.9685	488.15	0.8466
363.15	0.9653	493.15	0.8403
368.15	0.9618	498.15	0.8339
373.15	0.9583	503.15	0.8273
378.15	0.9547	508.15	0.8205
383.15	0.9509	513.15	0.8136
388.15	0.9471	518.15	0.8065
393.15	0.9431	523.15	0.7992
398.15	0.9391	528.15	0.7917
403.15	0.9348	533.15	0.7840
408.15	0.9306	538.15	0.7760
413.15	0.9262	543.15	0.7679
418.15	0.9217	548.15	0.7594
423.15	0.9170	553.15	0.7507
428.15	0.9123	558.15	0.7417
433.15	0.9074	563.15	0.7323
438.15	0.9025	568.15	0.7226
443.15	0.8974	573.15	0.7125
448.15	0.8923	578.15	0.7019
453.15	0.8870	583.15	0.6909
458.15	0.8816	593.15	0.6672
463.15	0.8761	603.15	0.6407
468.15	0.8705	613.15	0.6105
473.15	0.8647	623.15	0.5746
478.15	0.8588	633.15	0.5284

Table 3.3: Density Data from Standard Steam Tables for Water at a Pressure of 1 atm

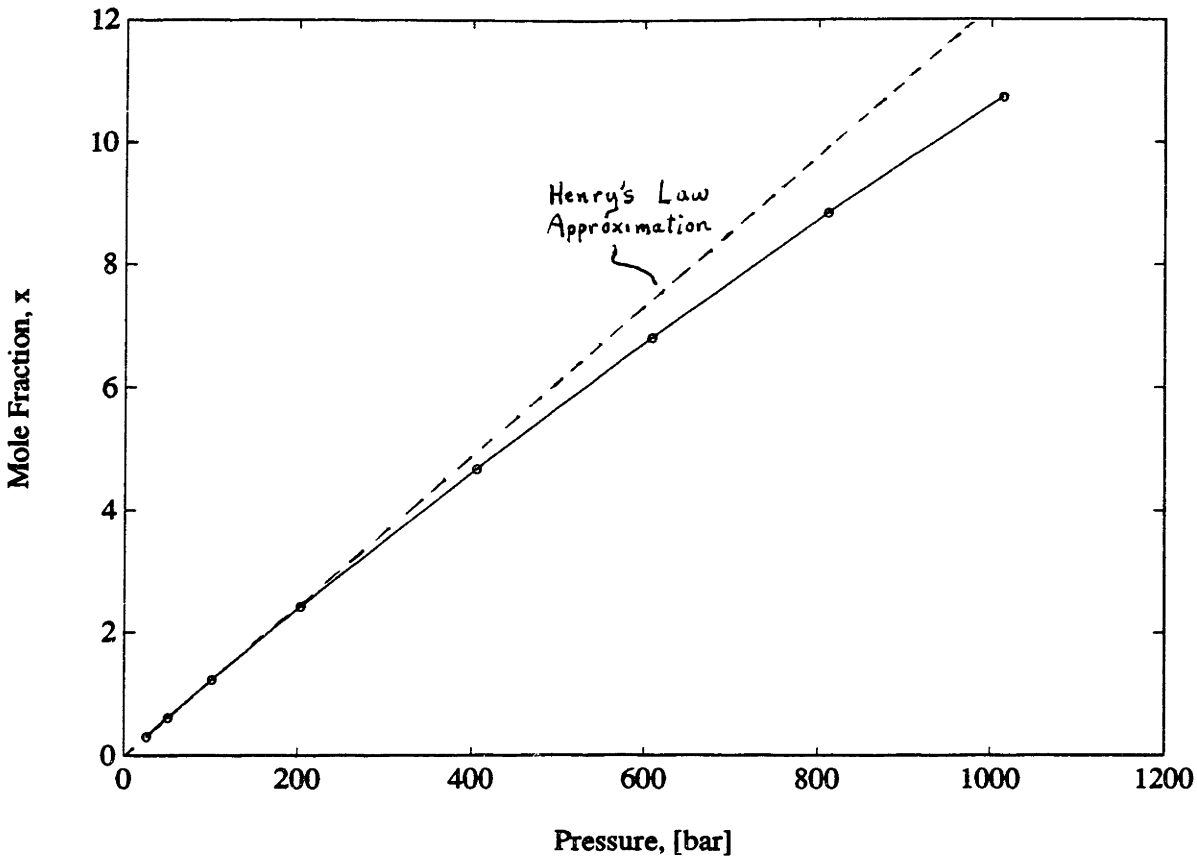

Source: [56] Wiebe, Gaddy, and Heins (1932)

Figure 3-5: Solubility of Hydrogen in 298.15K Water at Elevated Pressures

3.4.2 Solubilties at Pressures above 200 kPa

Gas solubilities increase in a slightly nonlinear manner with pressure at high pressures. However, at the relatively low pressures of interest for fuel cells, this is not an issue. Nonlinear behavior does not occur in water at pressures less than 50 bars; fuel cells typically operate below 10 bars. Thus, Henry's law can be assumed to apply for water in this pressure range. The complete range of applicability of Henry's law for the solubility of hydrogen and of oxygen in water can be observed in the representative plots shown in Figures 3-5 and 3-6.

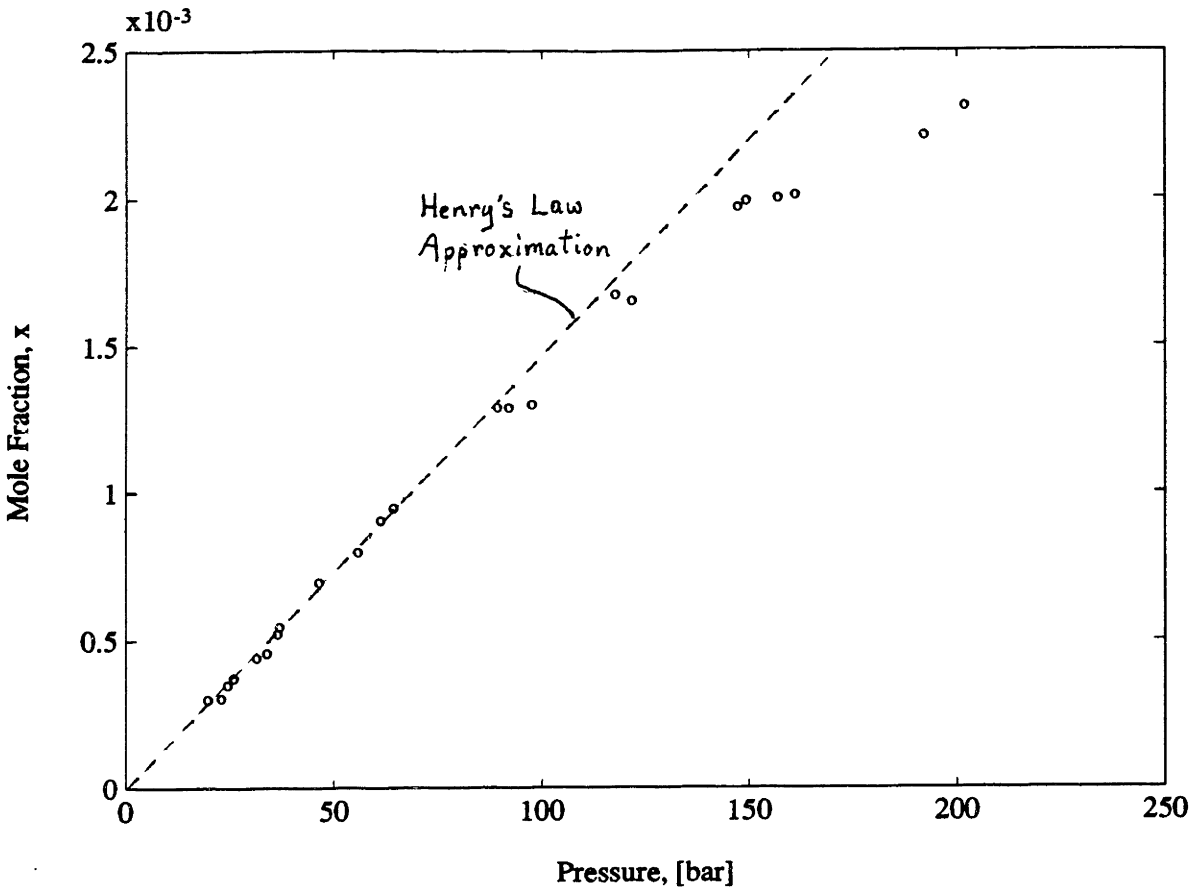

Source: [52] Stephan et. al (1956)

Figure 3-6: Solubility of Oxygen in 373.15K Water at Elevated Pressures

3.5 Solubility of Hydrogen and Oxygen in Selected Electrolytes

Unlike the solubility data for water, data for the solubility of hydrogen and oxygen in electrolyte solutions is sparse. According to Battino,

> The solubility of comparatively few systems is known with sufficient accuracy to enable a set of recommended values to be presented. This is true both of the measurement near atmospheric pressure and at high pressures. Although a considerable number of systems have been studied by at least two workers, the range of pressures and/or temperatures is often sufficiently different to make meaningful comparison impossible [7, p. xvii].

Thus, the data presented for the following electrolyte solutions can only be classed as tentative at best.

The data is preseented here in terms of the salting coefficient for sodium hydroxide, potassium hydroxide, and sulfuric acid because this is the way it was compiled by Battino and Young [7, 59]. Some data has been added to their data. Individual summaries of these studies and the methods by which the solubility data were converted to salting coefficients are detailed in Appendix A.

The salting coefficients for potassium hydroxide and sodium hydroxide are nearly linear functions of electrolyte concentration. Sulfuric acid, on the other hand, exhibits very nonlinear behavior (see Figure 3-7).

The solubility data for phosphoric acid, trifluoromethane sulfonic acid, and the molten carbonates were not converted to salting coefficients due to the lack of some key information and the fact that most of the data could be used directly to determine the gas solubility limits on current density.

T (K)	KOH	NaOH	H_2SO_4
293.15			0.0906[16]
294.15	0.123[33]		
298.15	0.137[25]	0.137[25]	0.0711[25]
	0.127[48]		
303.15	0.133[45]		0.0865[45]
313.15	0.130[48]		
318.15	0.132[33]		
323.15	0.169[14]	0.181[14]	0.075[14]
333.15	0.129[48]		
348.15	0.137[33]		
353.15	0.128[48]		
373.15	0.156[14]	0.190[14]	0.074[14]
	0.127[48]		
423.15	0.164[14]	0.179[14]	0.080[14]
473.15	0.151[14]	0.173[14]	0.074[14]
523.15	0.189[14]		0.074[14]

Sources:

[14] Bruhn, Gerlach, and Pawlek (1965)

[16] Christoff (1906)

[25] Geffcken (1904)

[33] Knaster and Apel'baum (1964)

[45] Ruetschi and Amlie (1966)

[48] Shoor, Walker, and Gubbins (1969)

Table 3.4: Hydrogen Salting Coefficients in 1M Aqueous Electrolytes at a Hydrogen Partial Pressure of 1 atm

T (K)	KOH	NaOH	H_2SO_4
273.15	0.18[20]		
288.15	0.190[25]	0.190[25]	0.105[25]
		0.158[58]	
294.15	0.160[33]		
298.15	0.177[25], 0.176[30]	0.180[25]	0.087[25]
	0.130[35], 0.171[27]	0.180[30]	
	0.180[48], 0.175[20]	0.160[58]	
308.15		0.167[58]	
310.2	0.167[1]	0.156[1]	0.0642[1]
313.15	0.168[48]		
318.15	0.160[33]		
323.15		0.185[14]	0.088[14]
333.15	0.159[48], 0.15[20]		
348.15	0.160[33]		
353.15	0.157[48]		
373.15	0.155[48]	0.171[14]	0.102[14]
423.15		0.187[14]	0.102[14]
473		0.187[14]	0.105[14]
523		0.167[14]	0.100[14]

Note: According to Battino, "MacArthur's value should be rejected." [7, p. 72].
Sources:

[14] Bruhn, Gerlach, and Pawlek (1965)
[16] Christoff (1906)
[1] CRC Handbook (1990-1991)
[20] Davis, Horvath, and Tobias (1967)
[25] Geffcken (1904)
[27] Gubbins and Walker (1965)
[30] Khomotuv and Konnik (1974)
[33] Knaster and Apel'baum (1964)
[35] MacArthur (1916)
[48] Shoor, Walker, and Gubbins (1969)
[58] Yasunischi (1978)

Table 3.5: Oxygen Salting Coefficients in Acids and Bases with Concentrations of 1 mol/l at Atmospheric Pressure

H_2SO_4 Conc. $[mol/l]$	Geffcken[25] $T = 288.15K$	Christoff[16] $T = 293.15K$	Bohr[11] $T = 294.2K$	Geffcken[25] $T = 298.15K$	Gubbins & Walker[27] $T = 298.15K$
0.245	0.134			0.115	
0.25					0.18
0.264	0.120			0.114	
0.489	0.109			0.099	
0.509	0.103			0.098	
0.915	0.102			0.085	
0.948	0.105			0.087	
1.474	0.100			0.088	
1.756	0.102			0.083	
2.06					0.092
2.45			0.082		
2.476	0.090				
2.647	0.092			0.078	
4.17					0.066
4.45			0.068		
4.63		0.063			
5.35			0.063		
9.52		0.038			
10.2			0.041		
10.3					0.0402
12.4			0.039		
12.7					0.0345
14.0					0.0312
14.8			0.030		
15.6					0.0223
17.1					0.0102
17.2			0.011		
17.9			0.003		0.0037

Table 3.6: Oxygen Salting Coefficients in Sulfuric Acid at Several Concentrations and Temperatures, with an Oxygen Partial Pressure of 1 atm

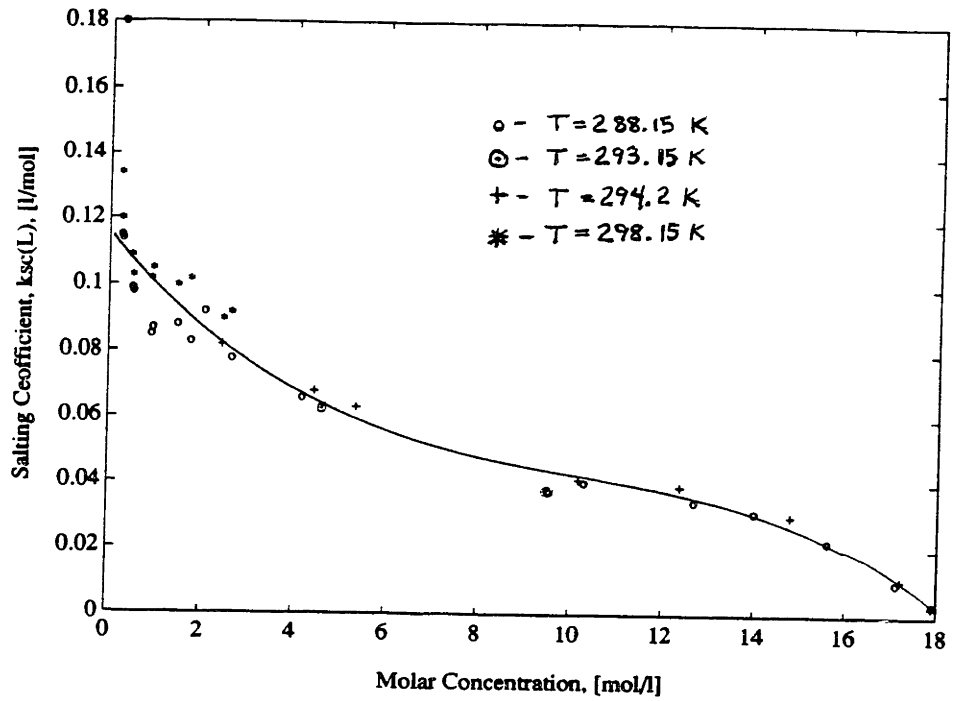

Sources: see Table 3.6

Figure 3-7: Nonlinear Relationship of the Salting Coefficient to the Concentration of Sulfuric Acid

Electrolyte	Temperature (K)	$10^6(C_{O_2})$ $(mol\ cm^{-3})$	$10^6 D_{O_2}$ $(mol\ cm^{-3})$
9.5 M TFMSA	306	4.20	7.9
(Electrode	316	4.11	10.6
diam 12.7μm)	330	3.50	14.6
	337	3.07	17.2
	343	3.41	20.4
	355	3.60	23.9
9.5 M TFMSA	325	3.16	15.0
(Electrode	341	3.19	19.5
diam 125 μm)	358	3.49	23.2

Source: Enayetullah et. al [22]

Table 3.7: Solubility of Oxygen in 9.5M Trifluoromethane Sulfonic Acid at an oxygen partial pressure of 1 atm

T(°C)	$10^7 c(mol\ cm^{-3})$	$10^6 D(cm^2 s^{-1})$
25	0.494	1.18
50	0.642	4.64
75	0.918	6.28
100	0.996	10.5
125	0.971	21.4
150	1.07	29.9

Source: Scharifker et. al [47]

Table 3.8: Oxygen Solubility and Diffusivity in 98% Phosphoric Acid at an Oxygen Partial Pressure of 1 atm

Po_2 (atm)	Pco_2 (atm)	10^6 S (mol fraction)
0.5	0.5	5.6
0.5	0.5	5.0
0.5	0.1	17.3
0.5	0.1	21.2
0.5	0.1	13.2
0.5	0.1	17.6
0.5	0.02	52.6
0.5	0.02	27.0
0.5	0.02	19.1
0.5	0.02	50.5
0.5	0.02	43.1
0.8	0.2	12.4*

*Data is for 50 m/o Li_2CO_3 - 50m/o K_2CO_3, from Literature [12]
Source: Smith et. al [51]

Table 3.9: Mole Fraction Solubility of Oxygen in Fused Lithium Carbonate - Potassium Carbonate at 923K

Chapter 4

Analysis

The solubility data was analyzed for each fuel cell system at a representative electrolyte concentration of 4M (molar) and a reactant gas partial pressure of 1 atm. The theoretical limiting current for each of the salting coefficient values from the tables were determined as follows: Recall from Section 3.3.11 that the salting coefficient is related to the Ostwald coefficient by

$$log \frac{L^o}{L} = c\, k_{sc_L}. \tag{4.1}$$

Thus, for a given electrolyte concentration

$$L = L^o\ 10^{-c\ k_{sc_L}}. \tag{4.2}$$

(Remember that the density correlation used to calculate L^o at high temperatures slightly overestimates the actual value for the data Bruhn found at temperatures of 473K and 523K.) The values found for the Ostwald coefficients were then plotted as a function of temperature or concentration.

The Ostwald coefficient was then converted to a mole per unit volume solubility. This was accomplished by first recalling that the Ostwald coefficient is the ratio of the volume of solute gas absorbed to the volume of solution it is absorbed by. Assuming that the solute gas behaves as an ideal gas, the mole per unit volume solubility can

be represented as

$$c_g = \frac{V_g(\frac{P}{RT})}{V_L} = \frac{PL}{RT}, \tag{4.3}$$

where c_g is the moles of solute gas per liter of solution.

The limiting influence of solubility on current density, in units of mA/cm^2, was then found from

$$i_{l,s} = F\ n\ c_g\ V\ \frac{1000mA}{A}\ \frac{1dm^3}{1000cm^3}, \tag{4.4}$$

where F is Faraday's constant ($F = 96,500\ Asec/equivalent$), n is the number of equivalents, and V is the velocity of the electrolyte in cm/sec. This equation can also be used to determine the minimum flow rate required to obtain a desired current density, if solubility is the limiting factor. This is given by

$$V_{min} = \frac{i_{desired}}{F\ n\ c_g}, \tag{4.5}$$

where $i_{desired}$ is at least the value obtainable in conventional fuel cells. For alkaline electrolytes, $i_{desired} \approx 470mA/cm^2$; for acid electrolytes, $i_{desired} \approx 325mA/cm^2$.

As discussed in Section 1.6.2, solubility alone may not be the only limiting factor. Electrochemical reactions and mass transfer may instead be limiting. However, since the electrochemical reactions are unaffected by reactant gas solubility, Holeshovsky's prediction that the electrochemical reaction is not limiting is assumed to hold. He concluded that mass transport appears to be the limiting factor [29]. Since mass transfer is influenced by solubility, it is analyzed here where possible.

Holeshovsky analyzed mass transport for the simple case of wire screen electrodes and the case of a porous foam electrode. Since screen electrodes are relatively easy to analyze, they were analyzed here. However, these are known to be poor electrodes. More work should be done to analyze mass transport with state-of-the-art electrodes.

The reactant gas mass transfer can be described by

$$Sh = A\ Re^b\ Sc^{0.33}, \tag{4.6}$$

where A and b are empirical constants, Sh is the Sherwood number, Re is the Reynolds

number, and Sc is the Schmidt number. For mass transport through screen electrodes, $Sh = kd/D$ and $Sc = \nu/D$, where k is the mass transport coefficient, d is the wire diameter, D is the diffusivity of the gas in the electrolyte, and ν is the electrolyte viscosity. The Reynolds number is given by

$$Re = \frac{(V/\epsilon)d}{\nu}, \tag{4.7}$$

where V is the electrolyte velocity, ν is the kinematic viscosity, and ϵ is a correction factor for the velocity of the electrolyte through the porous electrode. For a 180 mesh screen (180 wires per inch, or $N = 4.572$ wires per meter) with a wire diameter, d, of 5.84 x 10^{-5} m, $\epsilon = 1 - 2Nd = 0.174$.

The theoretical current density limit controlled by mass transfer for a given electrolyte is given by

$$i_{l,mt} = n\ F\ k\ (c_b - c_s)\ \frac{1000mA}{A}\ \frac{1dm^3}{1000cm^3}, \tag{4.9}$$

where c_b is the bulk concentration and c_s is the concentration on the electrode surface. For flooded flow fuel cell operation, $(c_b - c_s)$ can be approximated as $\frac{1}{2}c_g$, where c_g is the solubility of the gas in the electrolyte. Thus, for mass transport through screen electrodes,

$$i_{l,mt} = \frac{A\ n\ F\ D^{0.67}V^b c_g}{2\ d^{1-b}\epsilon^b\nu^{b-0.33}}. \tag{4.10}$$

This equation can be decomposed into three distinct components: a gas-electrolyte system contribution, a screen electrode geometry contribution, and an electrolyte velocity contribution. This can be summarized as follows

$$i_{l,mt} = K\ Ma\ Ge\ V^b, \tag{4.11}$$

where K is a constant which depends on the system selected (see equation 4.10). The

dependence upon the materials being considered is given by

$$Ma = \frac{c_g \, D^{0.67}}{\nu^{b-0.33}}. \tag{4.12}$$

The value of Ma is heavily dependent upon the operating conditions, as both solubility and diffusivity are both dependent upon temperature and electrolyte concentration, and solubility is dependent upon pressure. The dependence upon the screen geometry is given by the following grouping of variables:

$$Ge = \frac{1}{d^{1-b}(1 - 2 \, N \, d)^b}, \tag{4.13}$$

where N, the mesh number, is the number of wires per meter, and d is the diameter of the wire in meters. Thus, at a given temperature, pressure, and concentration, the mass transfer limit or current density for a selected gas-electrolyte system can be improved by changing the screen geometry (i.e. increasing Ge) or by increasing the velocity. The initial analyses were conducted for an arbitrary electrolyte velocity of 10 cm/s. Flooded flow fuel cells may be able to operate with electrolyte velocities as high as 50 cm/s, but this will need to be ascertained through research. A velocity of 10 cm/s is a conservative assumption.

Unless otherwise specified, all data is presented for gas partial pressures of 1 atm. For the alkaline and acid fuel cells, the solubility increases linearly with pressure as Henry's law is followed. Thus, at a partial pressure of 5 atm, the solubility would be equal to 5 times the value presented for 1 atm. As a result, the current density obtainable based upon solubility limitations would also be 5 times higher at 5 atm. Note that assessments of the mass transfer limits on current density were only determined for those studies which included diffusivity values with their solubility values.

4.1 Alkaline Electrolytes

4.1.1 Potassium Hydroxide

Significant amounts of data from a number of researchers are available for the solubility of hydrogen and oxygen in potassium hydroxide. However, these data vary study to study, and as a result, it is difficult to determine the actual solubility levels. The solubility of hydrogen and oxygen in 1M potassium hydroxide, in terms of the Ostwald coefficient, is presented as a funciton of temperature in Figure 4-1.

In the range of 273K to 373K, the solubility of hydrogen in terms of the Ostwald coefficient is most likely between 0.004 and 0.008, and the solubility of oxygen is between 0.005 and 0.01. The higher values for the solubility of oxygen occur at the low end of this temperature range. At temperatures above 373K, Bruhn et. al [14] found that the solubility of hydrogen increases to a value slightly greater than 0.014 at a temperature of 523K. It is likely that oxygen increases at higher temperatures as well; however, it cannot be assumed that the solubility of oxygen will increase with temperature at the same rate as does the solubility of hydrogen.

The gas solubility limits which correspond to the solubility data of Figure 4-1, corrected for a potassium hydroxide concentration of 4M, are presented in Figure 4-2. From these data, oxygen solubility for the temperatures shown apparently does not limit current density to a level below that attainable in conventional alkaline fuel cells. Hydrogen, on the other hand may limit current density to less than 470 mA/cm^2 at low temperatures and pressures with an electrolyte velocity of 10 cm/s. However, if the electrolyte velocity is increased to approximately 15 cm/s (which should be feasible), then hydrogen solubility would not be limiting, either.

Diffusivity values were presented by Davis et. al [20] as a function of molar concentration at temperatures of 298K and 333K. For a 4M solution, the diffusivity was given as approximately 0.87 x 10^{-9} and 2.3 x $10^{-9} m^2/s$, respectively, for these two temperatures. Bearing these values in mind, oxygen mass transfer limits were calculated at temperatures of 298K and 333K. The results are presented in Figure 4-3. Although the solubility values are lower at 333K than 298K, the diffusivity values

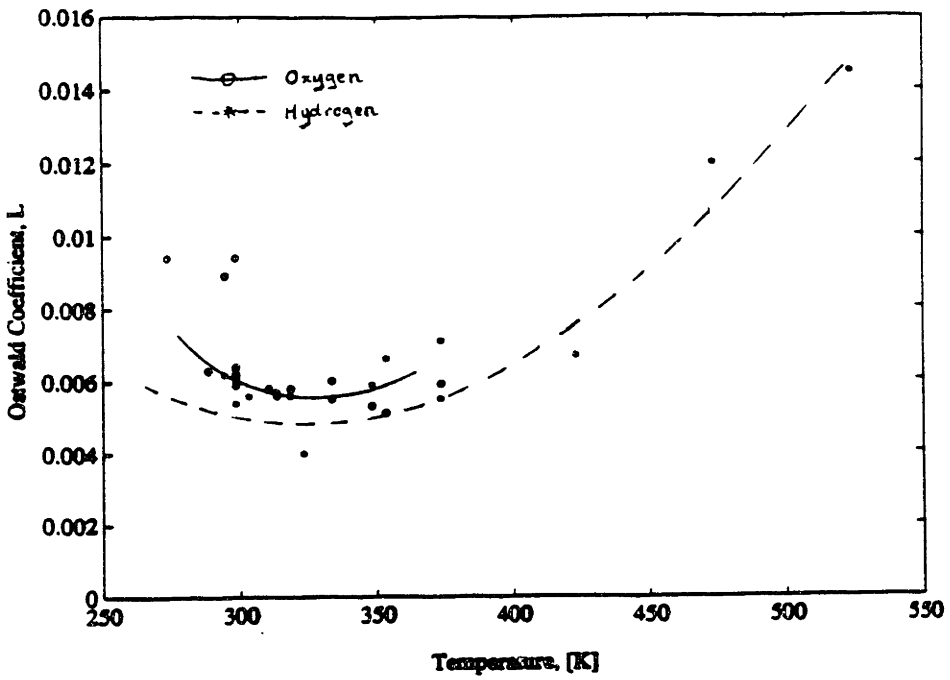

Sources: see Tables 3.5 and 3.4

Figure 4-1: Solubility of Oxygen and Hydrogen in 1M Potassium Hydroxide at a Partial Pressure of 1 atm

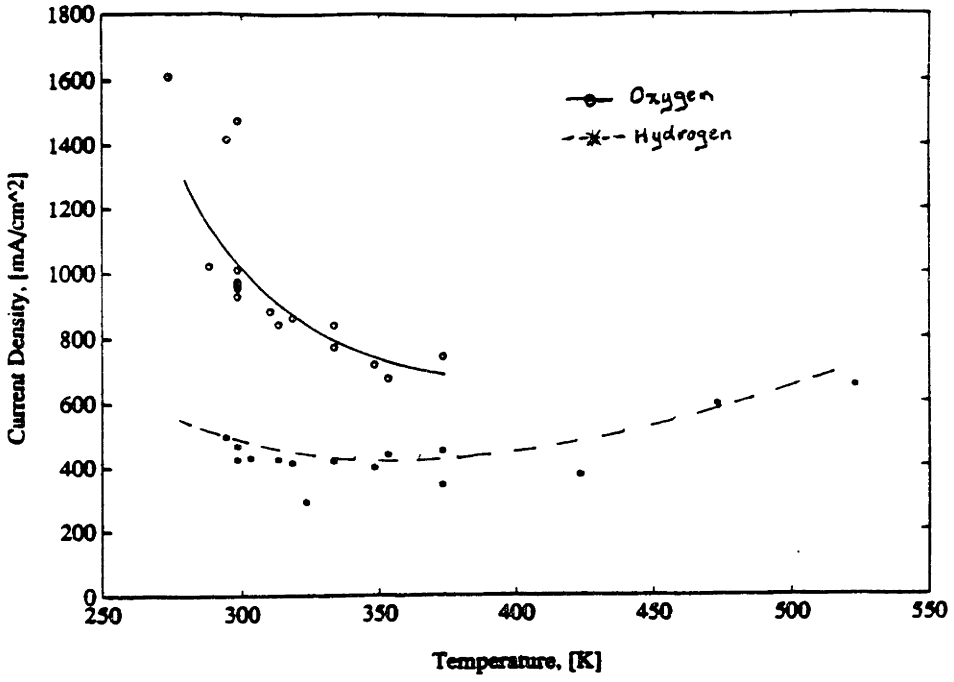

Figure 4-2: Reactant Gas Solubility Limitations on Current Density for 4M Potassium Hydroxide at a Partial Pressure of 1 atm

are sufficiently higher at 333K than 298K to offset the influence of the solubility values, resulting in a slightly higher limiting current density at 333K. However, all of these limiting current values are two orders of magnitude lower than is obtainable in conventional fuel cells. Since the mass transfer limiting current density is only a function of $V^{0.67}$, simply increasing the electrolyte velocity is not a feasible solution as velocities in excess of 1,000 cm/s would be required! Hence, operation at higher pressures (greater than 1 atm) and improving the electrode geometry will be required before the oxygen mass transfer rates in 4M potassium hydroxide for temperatures ranging from 298K to 333K, will be adequate.

4.1.2 Sodium Hydroxide

The hydrogen and oxygen solubility values found in the literature for sodium hydroxide were far more consistent than those for potassium hydroxide. The solubilties in terms of the Ostwald coefficient are presented in Figure 4-4. The data within the

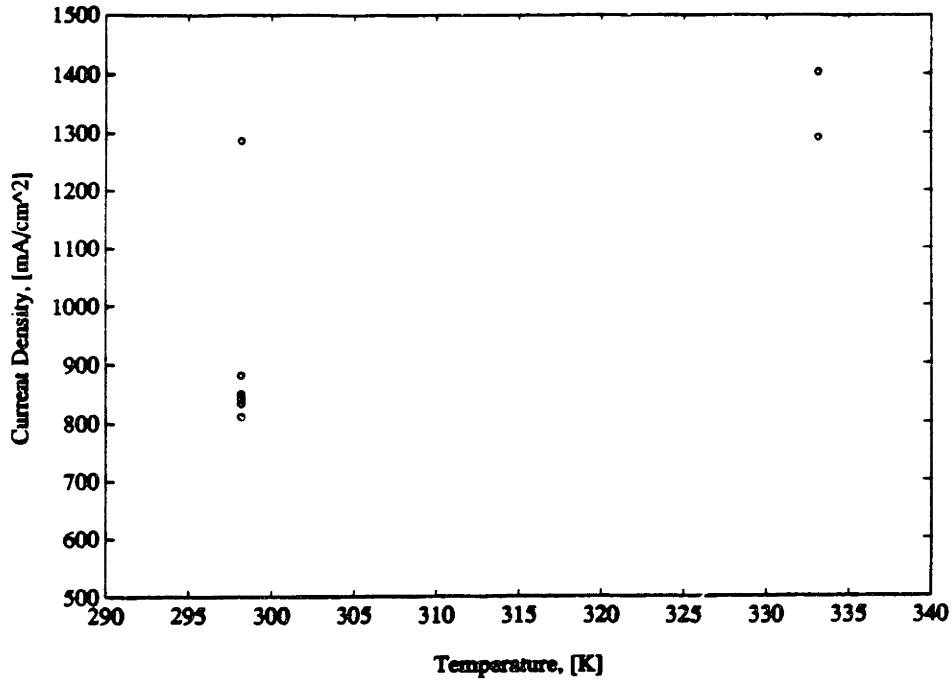

Figure 4-3: Oxygen Mass Transfer Limits on Current Density for 4M Potassium Hydroxide at a Partial Pressure of 1 atm

273K to 373K range proved to be quite similar to that of potassium hydroxide. At higher temperatures, however, the solubility in sodium hydroxide increases with temperature at a rate that is nearly twice that of potassium hydroxide, with an Ostwald coefficient for oxygen solubility of nearly 0.03 at a temperature of 523K.

Similar to 4M potassium hydroxide, the oxygen solubility definitely does not limit current density to less than 470 mA/cm^2 in 4M sodium hydroxide, as can be seen in Figure 4-5. Once again, by increasing the electrolyte velocity to 15-20 cm/s, the hydrogen solubility would not be limiting either. Thus, neither the hydrogen nor the oxygen solubility should detrimentally limit the obtainable current density. Since values for the diffusivity of hydrogen and oxygen in sodium hydroxide were not presented with any of the studies, no attempt was made to futhur assess mass transfer limitations.

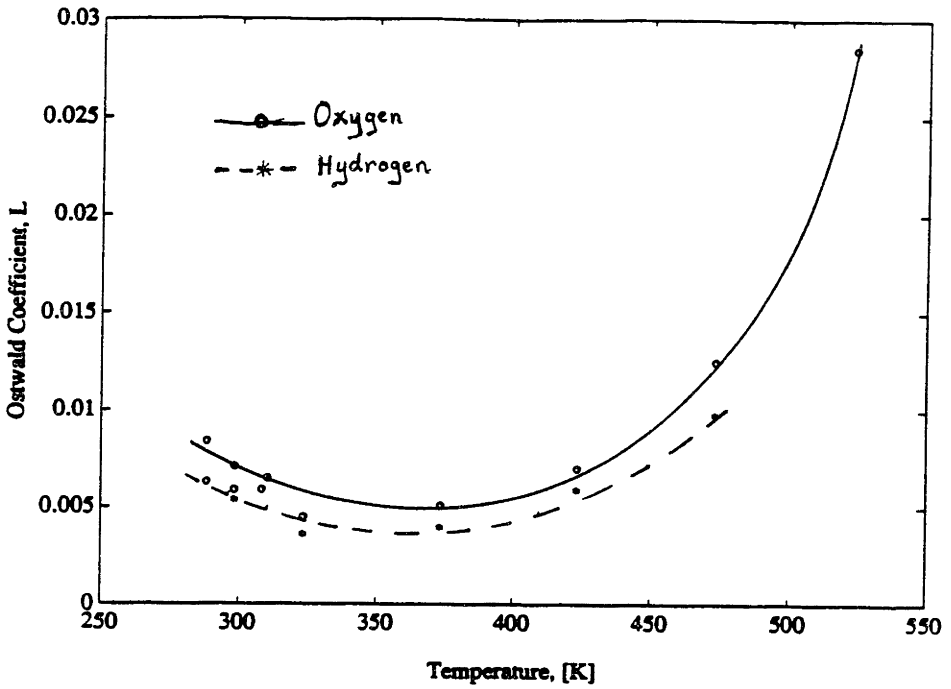

Sources: see Tables 3.5 and 3.4

Figure 4-4: Solubility of Hydrogen and Oxygen in 1M Sodium Hydroxide at a Partial Pressure of 1 atm

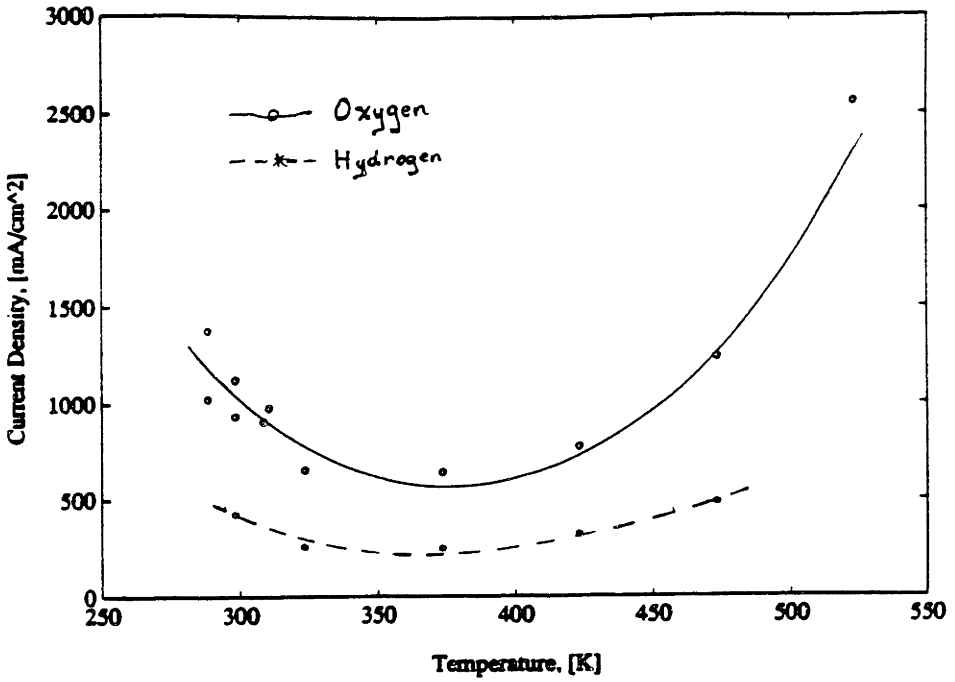

Figure 4-5: Reactant Gas Solubility Limitations on Current Density for 4M Sodium Hydroxide at a Partial Pressure of 1 atm

4.2 Acid Electrolytes

4.2.1 Phosphoric Acid

Three studies of the solubility of oxygen in phosphoric acid solutions were identified. The solubility values determined by Klinedinst et. al [32] differed significantly from the findings of Scharifker et. al [47] and Gubbins and Walker [27]. The three studies were conducted under vastly different conditions and are thus difficult to compare.

Gubbins and Walker assessed the solubility of oxygen in phosphoric acid at 298.15K over a range of concentrations of from 5 wt% to 85 wt%. They observed a near linear decrease in solubility with concentration over this range.

Klinedinst et. al measured the solubility in phosphoric acid concentrations ranging from 85 to 96 wt% and temperatures ranging from 373 to 423K. They concluded that oxygen solubility increases as a function of concentration, with the solubility being a stronger function of concentration at higher temperatures, until the solubility values

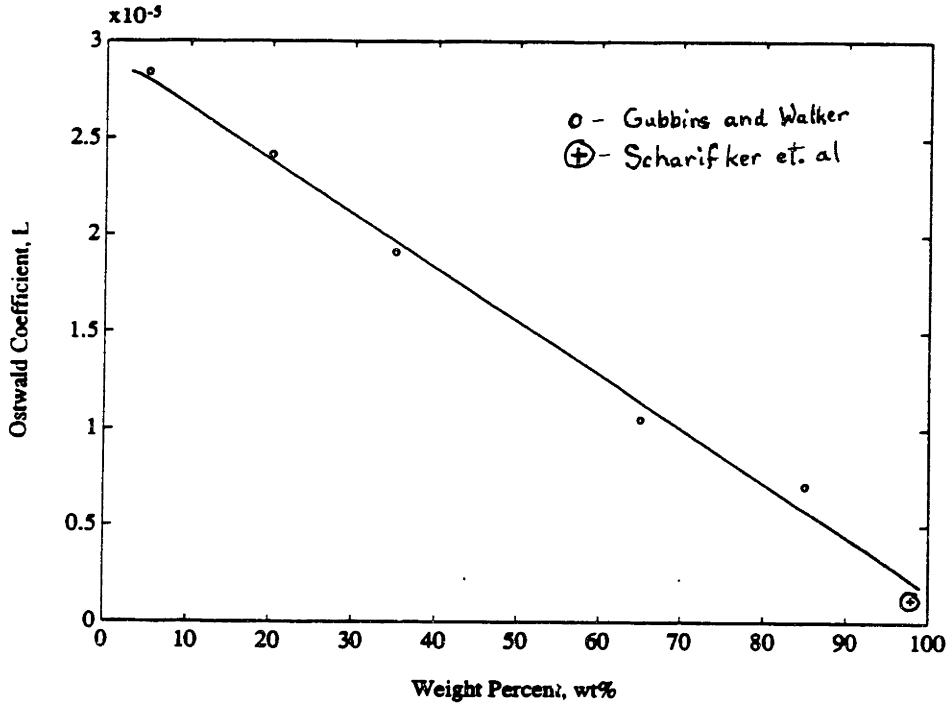

Sources: Scharifker et. al [47] and Gubbins and Walker [27]

Figure 4-6: Plot of the Agreement of the Values found for the Solubility of Oxygen in 98% Phosphoric Acid by Scharifker et. al and Gubbins and Walker for a Temperature of 298K and a Partial Pressure of 1 atm

become largely independent of temperature and converge at a concentration of about 96 wt%.

Scharifker et. al produced the first study of phosphoric acid solubilities at the taxing conditions under which today's fuel cells are operated. They utilized a microelectrode measurement technique to measure solubilities at temperatures ranging from 298K to 423K in 98 wt% acid. They found that the solubility reaches a maximum at a temperature of approximately 370K, above which the solubility does not vary with temperature. Their value at 298K fits fairly well with a linear fit to the values found by Gubbins and Walker. A plot of these oxygen solubility values at 298K is shown in Figure 4-6. By contrast, Figures 4-7 and 4-8 indicate the discrepancy of the values Scharifker et. al with the values of Klinedinst et. al.

This discrepenancy in solubility results is difficult to explain in and of itself. However, both research groups measured oxygen diffusivity as well as solubility. It

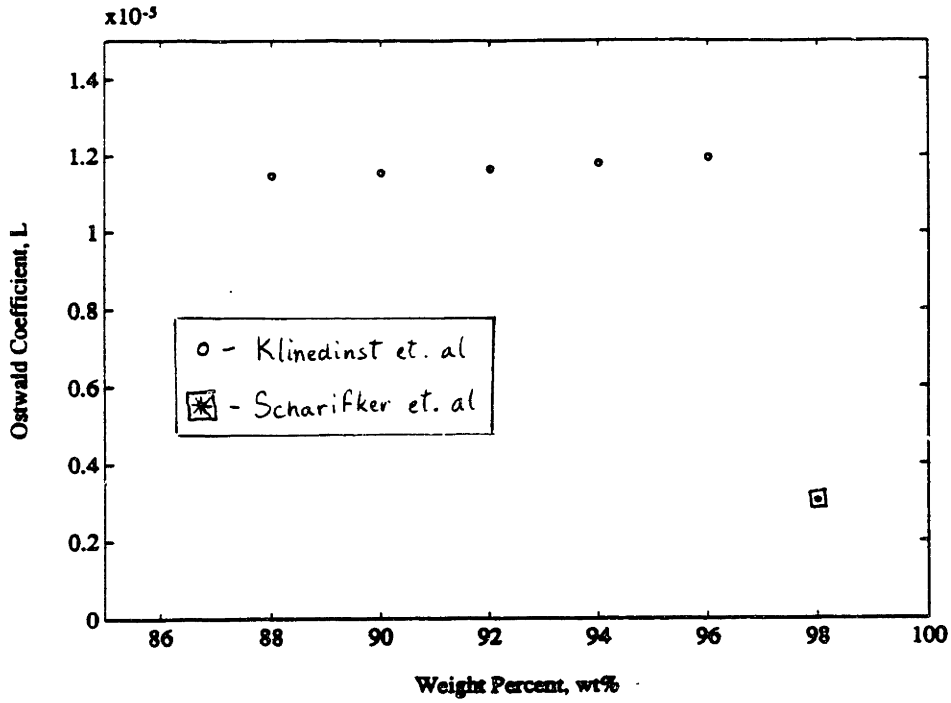

Sources: Scharifker et. al [47] and Klinedinst et. al [32]

Figure 4-7: Plot of the Discrepancy in the Values found for the Solubility of Oxygen in 98% Phosphoric Acid by Scharifker et. al and Klinedinst et. al for a Temperature of 373K and a Partial Pressure of 1 atm

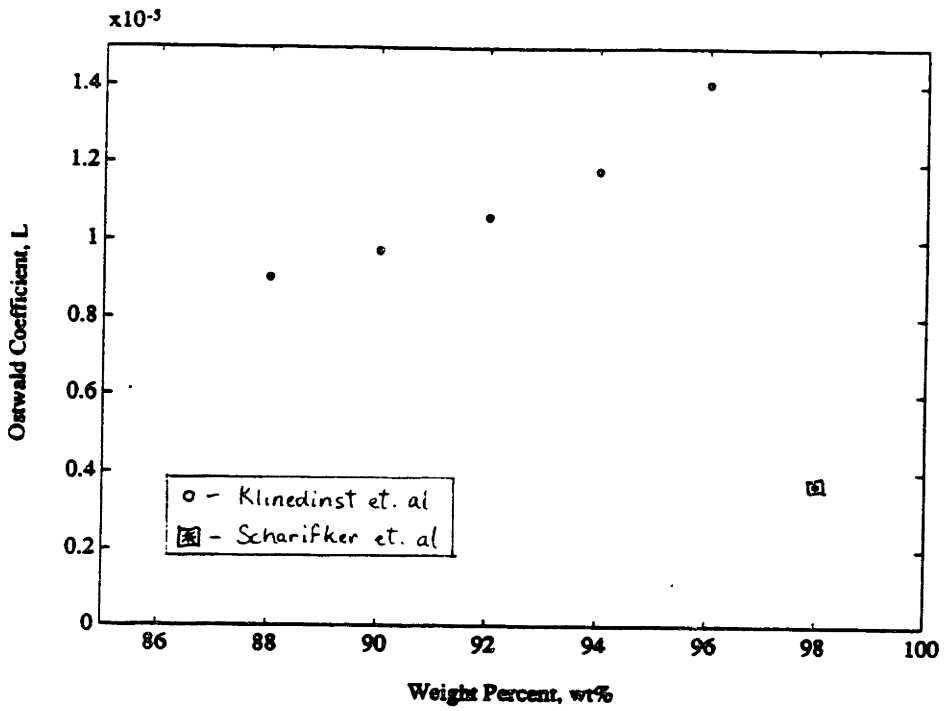

Sources: Scharifker et. al [47] and Klinedinst et. al [32]

Figure 4-8: Plot of the Discrepancy in the Values found for the Solubility of Oxygen in 98% Phosphoric Acid by Scharifker et. al and Klinedinst et. al for a Temperature of 423K and a Partial Pressure of 1 atm

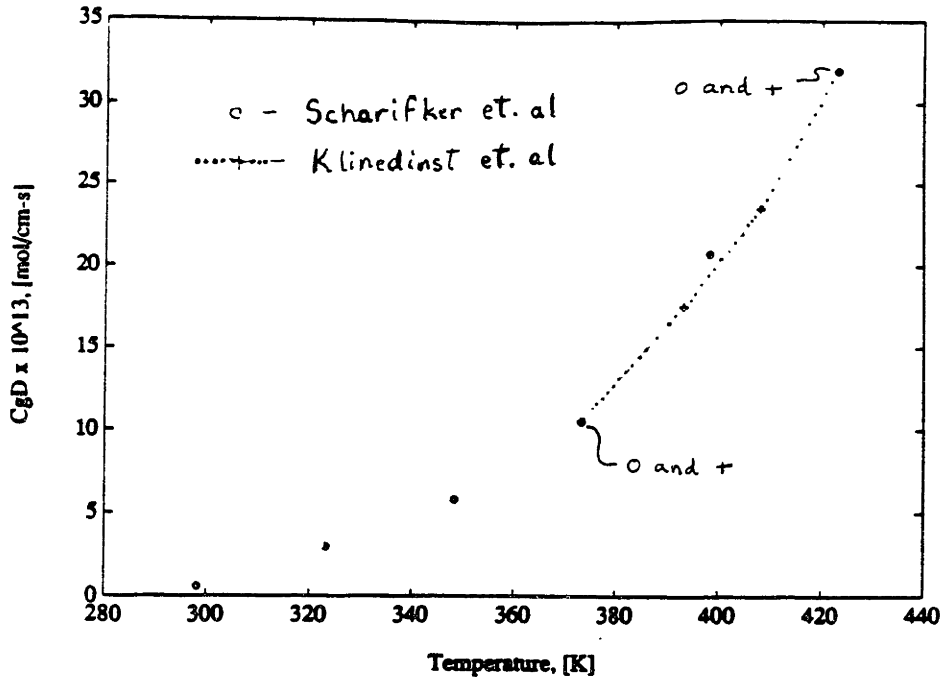

Sources: Scharifker et. al [47] and Klinedinst et. al [32]

Figure 4-9: Plot of the Product of the Experimental Oxygen Solubility and Diffusivity Values of Scharifker et. al with that of Klinedinst et. al for a 98 wt% Concentration at a Partial Pressure of 1 atm

is interesting to note that while the solubilities and diffusivities obtained by the two groups are very different, the product of their diffusivity and solubility values, when Klinedist's data is extrapolated to a concentration of 98 wt%, is nearly identical. This is shown in Figure 4.2.1.

The findings of Scharifker et. al appear to be the most reliable and significant. Limiting current density calculations have been carried out for these solubility values. The results are shown in Figure 4-10. In order to attain a current density of 470 mA/cm^2, an electrolyte velocity of about 17 cm/sec would be required at a temperature of 298K, while at a temperature of 423K, an electrolyte velocity of only about 8 cm/sec would be required. Thus, oxygen solubility does not limit current density to levels below those obtainable in conventional phosphoric acid flooded flow fuel cells.

However, the low values of solubility and diffusivity combine for a very low theoretical mass transfer current density. The theoretical current densities at a velocity of

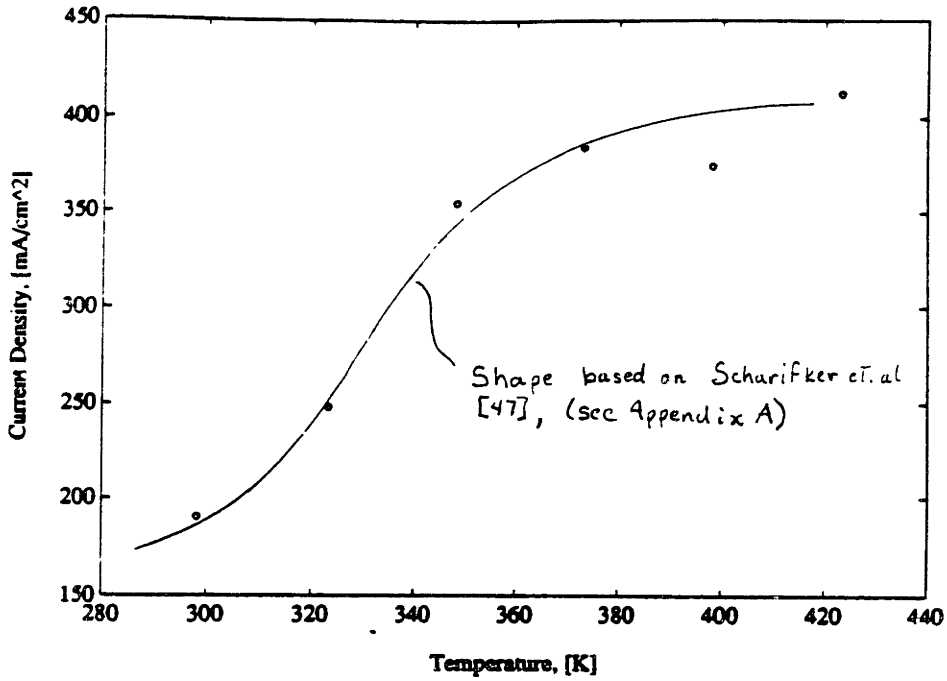

Figure 4-10: The Limits of Oxygen Solubility on the Current Density Obtainable with 98 wt% Phosphoric Acid at a Partial Pressure of 1 atm

10 *cm/sec* are shown in Figure 4-11. These values are very low. Increasing pressure and velocity will not be enough to improve the oxygen mass transfer-limited current densities to adequate levels. High specific surface area electrodes would be used in pratical application of flooded flow phosphoric acid fuel cells.

4.2.2 Trifluoromethane Sulfonic Acid

Trifluoromethane sulfonic acid (TFMSA) has been proposed as an alternative to phosphoric acid for conventional fuel cells because of its superior oxygen reduction kinetics. This property makes TFMSA electrolytes even more attractive for flooded flow fuel cell applications. Enayetullah et. al [22] used a microelectrode technique to investigate the solubility and diffusivity of oxygen in 9.5M TFMSA over a temperature range of 306K to 358K.

The solubility in terms of the Ostwald coefficient is presented in Figure 4-12. These solubilities are more 20 times the maximum oxygen solubility in 98% phosphoric acid.

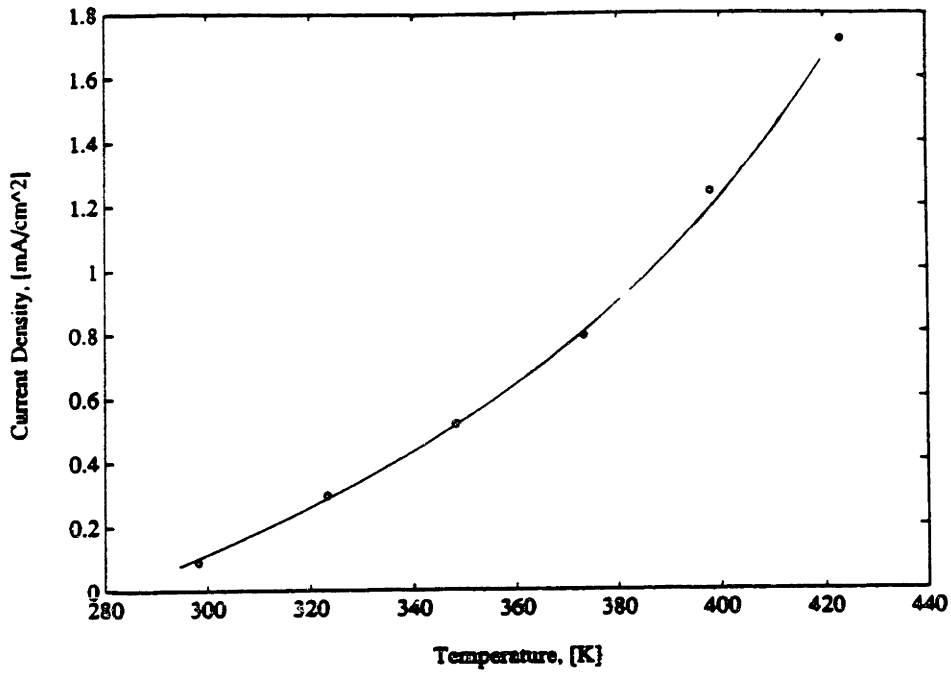

Figure 4-11: Mass Transfer Limits on the Current Density Obtainable with a 98 wt% Phosphoric Acid at a Partial Pressure of 1 atm

These values translate to the oxygen solubility limits on current density shown in Figure 4-13.

The diffusivity of oxygen in TFMSA is also significantly higher than in phosphoric acid. As a result, the oxygen mass transfer limitations allow for significantly higher current densities. The results are shown in Figure 4-14. These current densities are only 7-10 times lower than those obtainable in conventional phosphoric acid fuel cells. While velocity increases alone are probably not enough to provide sufficient current densities (a velocity of at least 180 cm/s would be required), a combination of increases in electrode area, fluid velocity, and/or oxygen partial pressure could feasibly achieve current densities equal to those of conventional fuel cells. For example, wire screen electrodes at a partial pressure of 4 atm and a velocity of 25 cm/s, a maximum current density of nearly 350 mA/cm^2 would be obtainable for the data point at 355K.

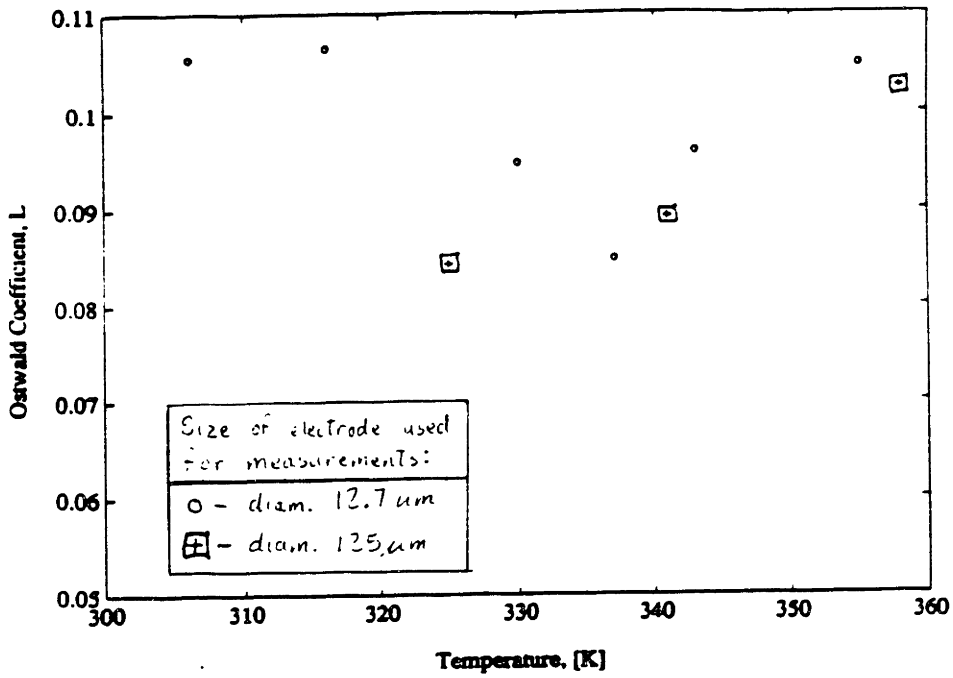

Source: Enayetullah et. al [22]

Figure 4-12: Solubility of Oxygen in 9.5M TFMSA at a Partial Pressure of 1 atm

4.2.3 Sulfuric Acid

The solubility of hydrogen and oxygen in sulfuric acid has been studied by a number of researchers. It has been found that the salting coefficient is a nonlinear function of sulfuric acid concentration. The solubility of hydrogen and oxygen in approximately 1M sulfuric acid is shown in Figure 4-15. At temperatures between 273K and 373K, the solubility of oxygen was 5-25 times greater than the corresponding values for 98% phosphoric acid electrolytes, but about 3-5 times less than the corresponding values for 9.5M TFMSA. The influence of sulfuric acid concentration on the solubility of oxygen is shown in Figure 4-16. Note that the oxygen solubility reaches a minimum at a sulfuric acid concentration of approximately 13 mol/l.

The gas solubility limitations on current density for 1M sulfuric acid are shown in Figure 4-17, and for 4M sulfuric acid in Figure 4-18. The values for the 4M sulfuric acid were calculated assuming that the salting coefficient varies linearly with sulfuric acid concentration over the range from 1M to 4M. This assumption can be verified by

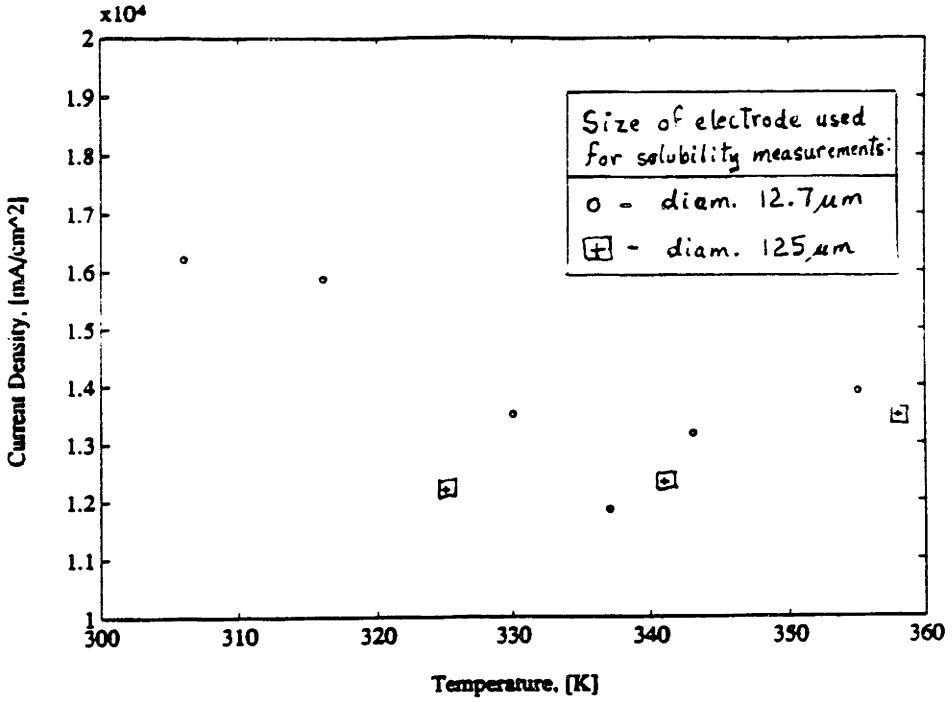

Figure 4-13: Oxygen Solubility Limitations on Current Density for 9.5M TFMSA at a Partial Pressure of 1 atm

observing the linear behavior of the solubility in this range in Figure 4-16. The limits on current density imposed by sulfuric acid over this entire concentration range are shown in Figure 4-19. For this concentration and temperature range, it is apparent that the solubility of hydrogen and oxygen will not limit the current density below the range obtainable by conventional fuel cells

4.3 Molten Carbonate Electrolytes

Two studies of the solubility of oxygen in molten carbonates were found. Andresen [3] found the solubility of oxygen in molten sodium carbonate to be 2.3 x $10^{-6} mol/cm^3$. With an electrolyte velocity of 10 cm/s, this corresponds to an oxygen solubility limiting current density of 8878 mA/cm^2. Thus oxygen solubility will not be a pose problem in terms of solubility limits on the obtainable current density. In the second study, Smith et. al [51] determined the mole fraction solubility of oxygen in fused

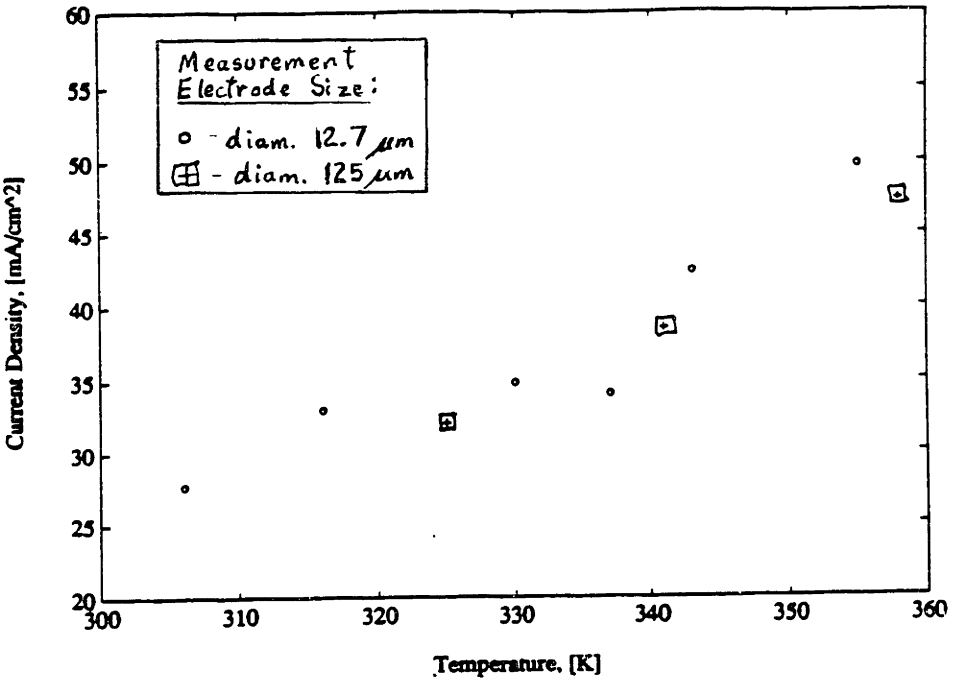

Figure 4-14: Oxygen Mass Transfer Limitations on Current Density for 9.5M TFMSA at a Partial Pressure of 1 atm

lithium carbonate - potassium carbonate. Their solubility data were quite scattered (see Appendix A). No further analysis was conducted on Smith et. al's solubility data as the density of this mixture was unknown and the mole fraction could not be converted to a mole per unit volume solubility.

Both research groups concluded that the solubility of oxygen in molten carbonates does not follow Henry's law. They suggest that this could be linked to the high temperature formation of peroxide and superoxide from molecular oxygen.

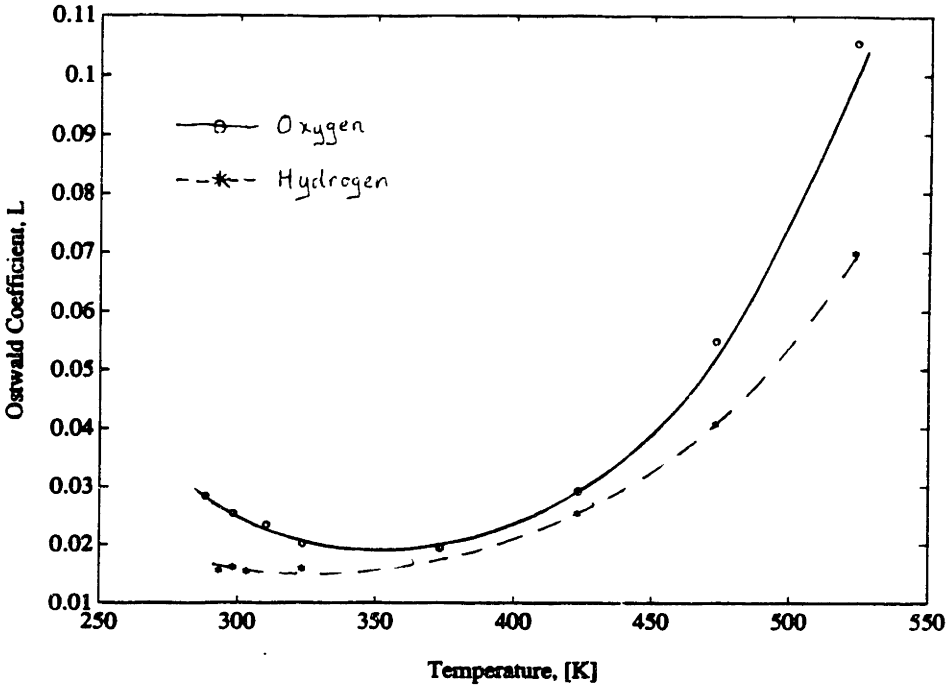

Figure 4-15: Solubility of Hydrogen and Oxygen in 1M Sulfuric Acid at a Partial Pressure of 1 atm

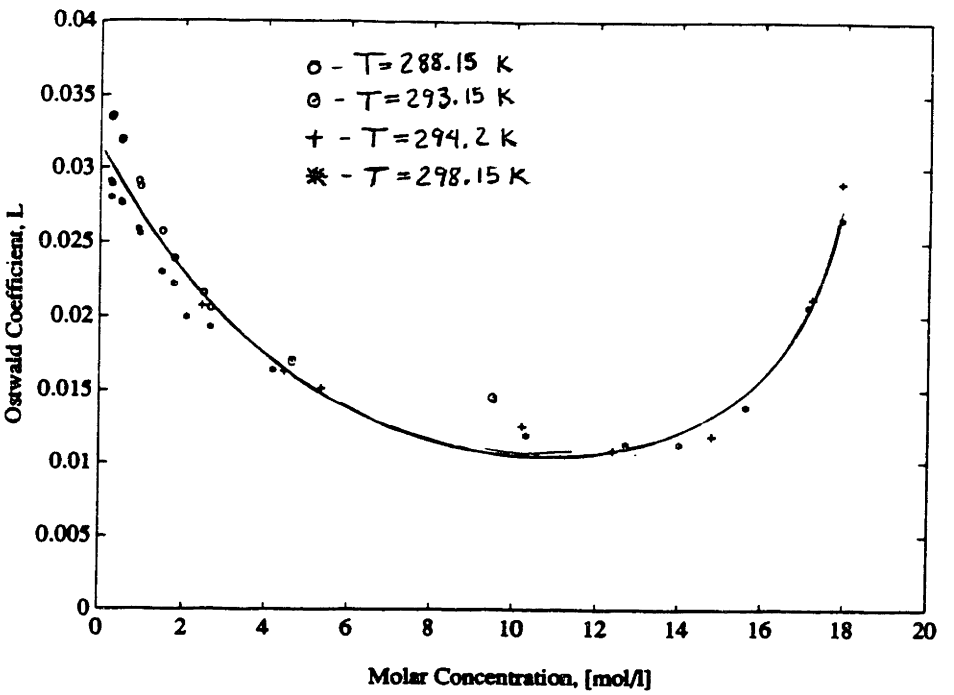

Figure 4-16: Influence of Sulfuric Acid Concentration on the Solubility of Oxygen at a Partial Pressure of 1 atm

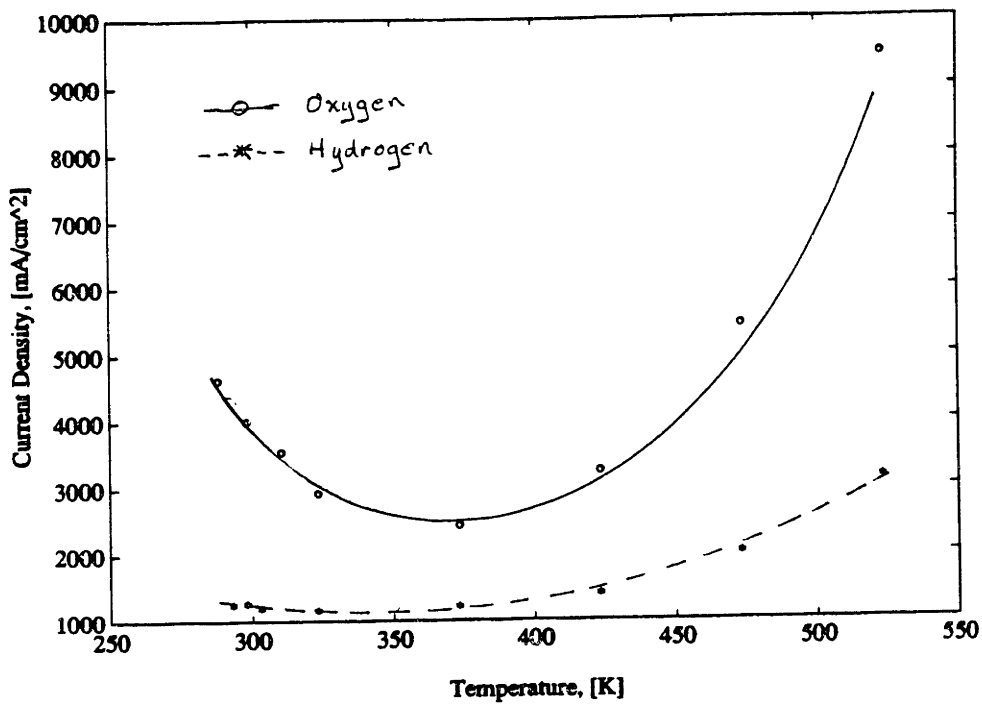

Figure 4-17: Gas Solubility Limitations on Current Density for 1M Sulfuric Acid at a Partial Pressure of 1 atm

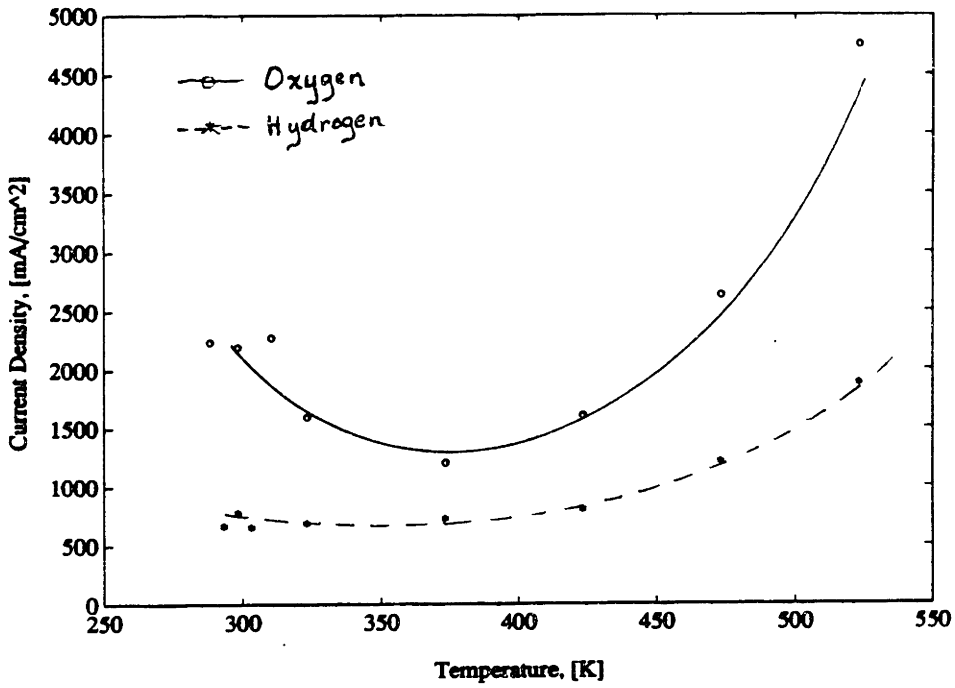

Figure 4-18: Gas Solubility Limitations on Current Density for 4M Sulfuric Acid at a Partial Pressure of 1 atm

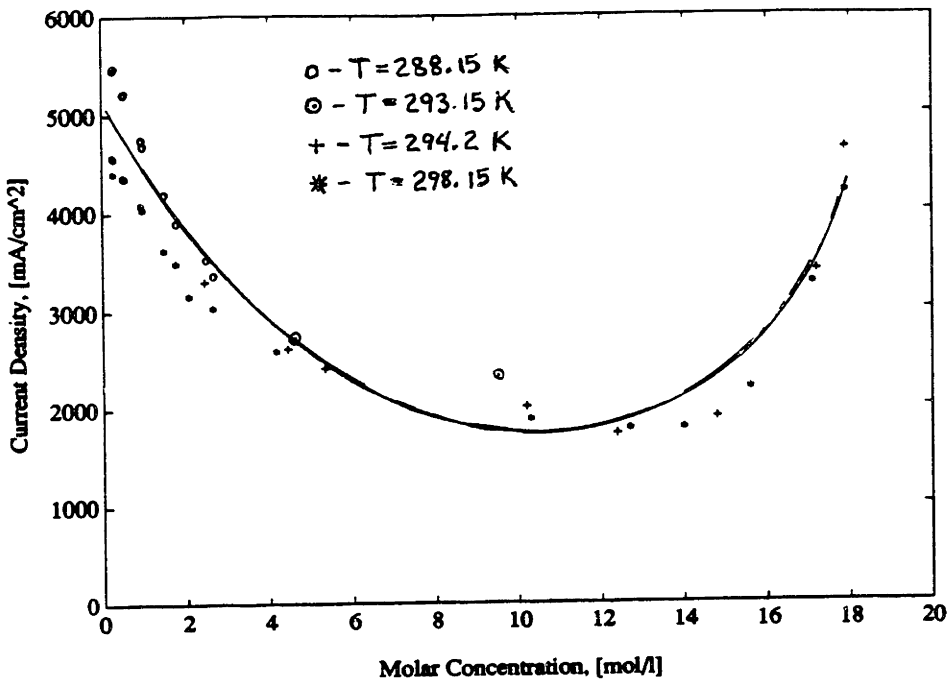

Figure 4-19: Gas Solubility Limitations on Current Density for Varying Concentrations of Sulfuric Acid at a Partial Pressure of 1 atm

Chapter 5

Conclusions and Recommendations

Fuel cells have the potential to play a significant role in the determination of the electric power supply mix of the future. The flooded flow fuel cell has the potential to improve the performance of fuel cells, and thus better postion them for commercialization. The goal of this study and analysis of available literature was to determine if the solubility of hydrogen or oxygen in fuel cell electrolytes limits current density to unacceptable levels. A second goal of the analysis was to identify the electrolytes which have the best solubility characteristics.

This analysis clearly indicates that the solubility of hydrogen and oxygen in the electrolyte solutions of concern does not severley limit the current densities obtainable in flooded flow fuel cells; however, some electrolytes offer better solubility characteristics than others. Since the solubility is important for mass transfer limitations on current density as well, it is important to utilize electrolytes which will not severely limit mass transfer as well.

Trifluoromethane sulfonic acid and sulfuric acid proved to be the least limiting as far as solubility is concerned. Although inadequate diffusivity data was available for a thorough analysis of all electrolytes, TFMSA also proved to be the only electrolyte to be marginally feasible from a mass transfer limiting perspective. Obtainable current densities in potassium hydroxide and phosphoric acid, although not limited to

unacceptable levels by oxygen solubility alone, were shown to be severely limited by oxygen mass transfer, which is a strong function of oxygen solubility.

Thus, for separate feed operation, TFSMA promises to at least be a good catholyte. Since no data was identified for the solubility of hydrogen in TFSMA, more work needs to be done to assess the feasability of TFSMA (as well as the other electrolytes) as an anolyte. Sulfuric acid was shown to have better hydrogen and oxygen solubilities than both potassium hydroxide and sodium hydroxide. Thus, based upon the available solubility data, it is the leading candidate for mixed feed operation. Without significant improvements in electrode geometry, it appears that the alkaline electrolytes and phosphoric acid will be less desirable than TFSMA and sulfuric acid.

Appendix A

Unconverted Solubility Data

Source: [27] Gubbins and Walker (1965)

Method(s): Gas chromatography

Solute(s): O_2

Electrolyte(s): KOH, H_3PO_4, and H_2SO_4

Concentration (Range): 0-40 wt%, 0-100 wt%, 0-100 wt%

Temperature (Range): 25°C and -30°C

Findings: Data taken from plots

Solubility in terms of the Kuenen coefficient, S x 10^4, was presented graphically

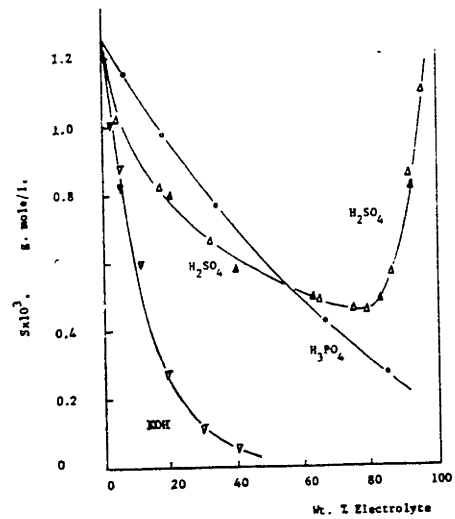

Fig. 2. Solubility of O_2 at 25°C: ○, experimental results for H_3PO_4; △, experimental results for H_2SO_4; ▽, experimental results for KOH; ▲, results of Bohr for H_2SO_4 (corrected to 1 atm assuming Henry's law); ▼, results of Geffcken for KOH.

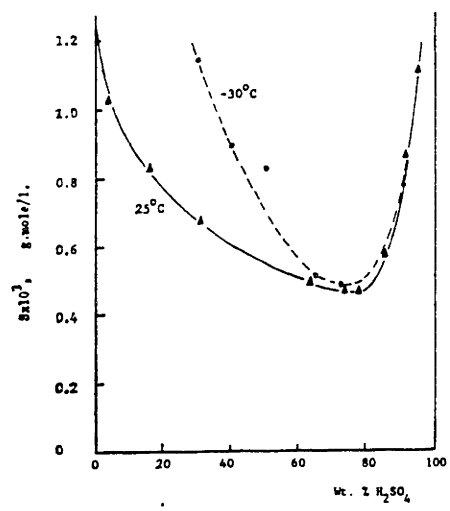

Fig. 3. Solubility of O_2 in H_2SO_4 at 25° and —30°C

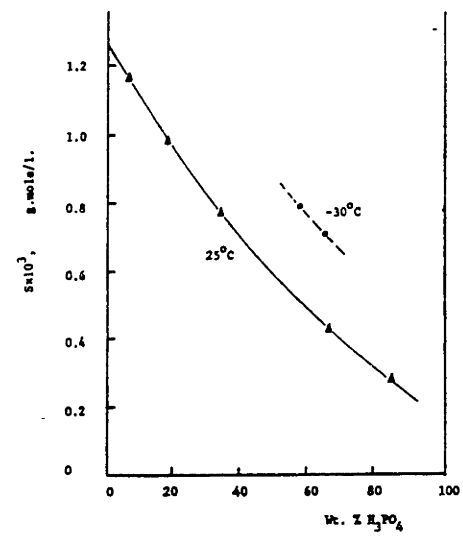

Fig. 4. Solubility of O_2 in H_3PO_4 at 25° and —30°C

Wt %	KOH 25°C	H_2SO_4 25°C	H_3PO_4 25°C	H_3PO_4 −30°C
5	0.88	1.02	1.16	
10	0.60			
18		0.82		
20	0.27		0.99	
30	0.11			
33		0.67		
35			0.78	
40	0.06			
58				0.79
64				0.70
65		0.49	0.43	
75		0.46		
80		0.46		
85			0.29	
86		0.57		
92		0.85		
96		1.09		

Source: [47] Scharifker, Zelenay, and Bockris (1987)

Method(s): Microelectrode techniques

Solute(s): O_2

Electrolyte(s): H_3PO_4

Concentration (Range): 98 wt.%

Temperature (Range): 25 - 150 °C

Findings: Oxygen solubility and diffusivity in 98% H_3PO_4

T(°C)	$10^7 c(molcm^{-3})$	$10^6 D(cm^2 s^{-1})$
25	0.494	1.18
50	0.642	4.64
75	0.918	6.28
100	0.996	10.5
125	0.971	21.4
150	1.07	29.9

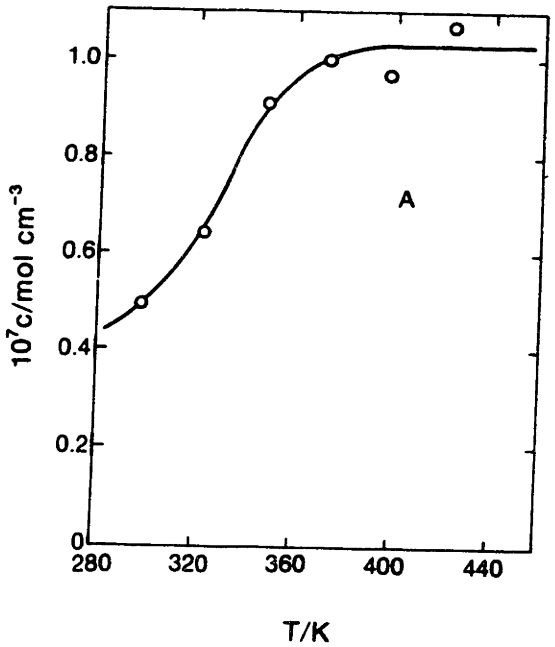

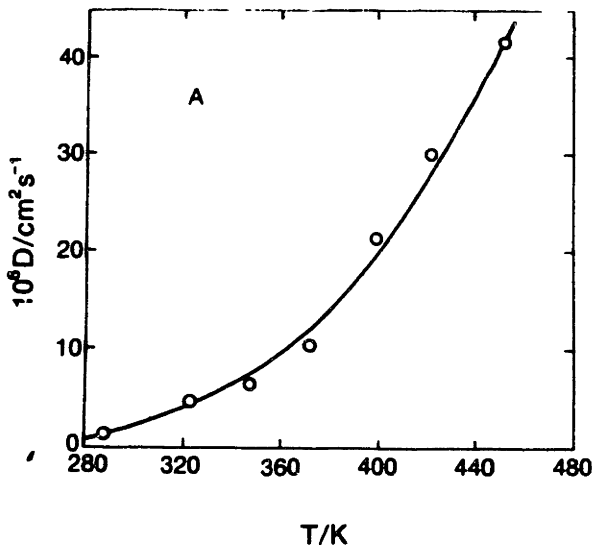

Oxygen solubility in 98% phosphoric acid. Saturation concentration of oxygen as a function of temperature (left)

Oxygen diffusivity in 98% phosphoric acid. Diffusion coefficient of oxygen as a function of temperature (right)

Source: [32] Klinedinst, Bett, and MacDonald (1974)

Method(s): Electrode technique

Solute(s): O_2

Electrolyte(s): H_3PO_4

Concentration (Range): 86 - 95.6 wt.%

Temperature (Range): 100 - 150 °C

Findings: Graphical form

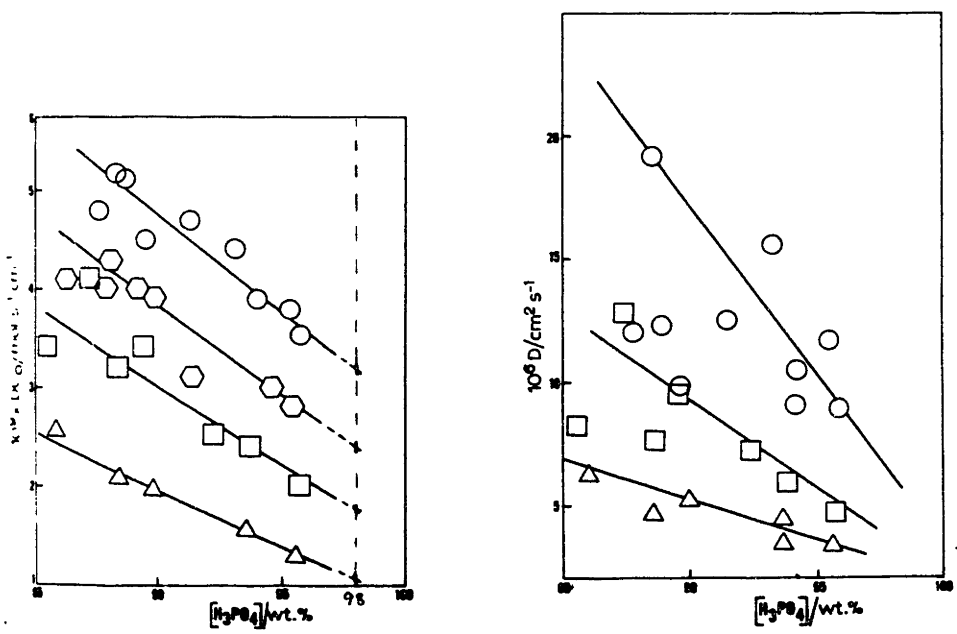

Fig. 2. Oxygen diffusion coefficient–solubility product (corrected to 1 atm. oxygen partial pressure) *vs.* H_3PO_4 concentration. (△) 100°C, (□) 120°C, (○) 135°C, (○) 150°C.

Fig. 3. Oxygen diffusion coefficient *vs.* H_3PO_4 concentration. (△) 100°C, (□) 120°C, (○) 150°C.

Source: [3] Andresen (1979)

Method(s): Manometric technique

Solute(s): O_2

Electrolyte(s): molten Na_2CO_3

Concentration (Range): given in terms of pressure

Temperature (Range): 872°C

Findings: O_2 dissolution

Δp (Torr)	Pumping time (min)	Total pressure (Torr)	c x 10^6 (mole-cm^{-3})
33.52	60	717.0	2.92
50.20	295	677.5	4.39
59.28	235	566.5	5.16
25.96	55	714.5	2.27
29.10	58	688.5	2.55
24.52	60	699.5	2.15
21.56	70	684.5	1.88
24.04	65	461.5	2.09
21.04	60	452.5	1.82
17.98	72	269.5	1.23
18.65	60	312.5	1.61

Solubility = 2.3 x 10e-6 mol/cm3, which translates to L = 2.16 x 10e-7

Source: [22] Enayetullah, DeVilbiss, and Bockris (1989)

Method(s): Microelectrode technique

Solute(s): O_2

Electrolyte(s): TFMSA

Concentration (Range): 9.5 M

Temperature (Range): 33 - 85 °C

Findings: Solubility of O_2 in TFMSA

Electrolyte	Temperature (K)	$10^6(C_{O_2})$ $(mol\ cm^{-3})$	$10^6 D_{O_2}$ $(mol\ cm^{-3})$
9.5 M TFMSA (Electrode diam 12.7μm)	306	4.20	7.9
	316	4.11	10.6
	330	3.50	14.6
	337	3.07	17.2
	343	3.41	20.4
	355	3.60	23.9
9.5 M TFMSA (Electrode diam 125 μm)	325	3.16	15.0
	341	3.19	19.5
	358	3.49	23.2

Source: [51] Smith, Vogel, and Kopelner (1982)

Method(s): Saturation Method

Solute(s): 62 mol percent (m/o)

Electrolyte(s): $Li_2CO_3 - K_2CO_3$

Concentration (Range): 62 m/o Li_2CO_3 - 38 m/o K_2CO_3

Temperature (Range): 650°F

Findings: Oxygen solubilities

Po_2 (atm)	Pco_2 (atm)	10^6 S (mol fraction)
0.5	0.5	5.6
0.5	0.5	5.0
0.5	0.1	17.3
0.5	0.1	21.2
0.5	0.1	13.2
0.5	0.1	17.6
0.5	0.02	52.6
0.5	0.02	27.0
0.5	0.02	19.1
0.5	0.02	50.5
0.5	0.02	43.1
0.8	0.2	12.4*

*Data is for 50 m/o Li_2CO_3 - 50m/o K_2CO_3, from Lit.

Source: [20] Davis, Horvath, and Tobias (1967)

Method(s): Van Slyke technique and Hildebrand Method

Solute(s): O_2

Electrolyte(s): KOH

Concentration (Range): 0-12 N

Temperature (Range): 0, 25 and 60°C

Findings: Oxygen solubilities and diffusivities were presented graphically

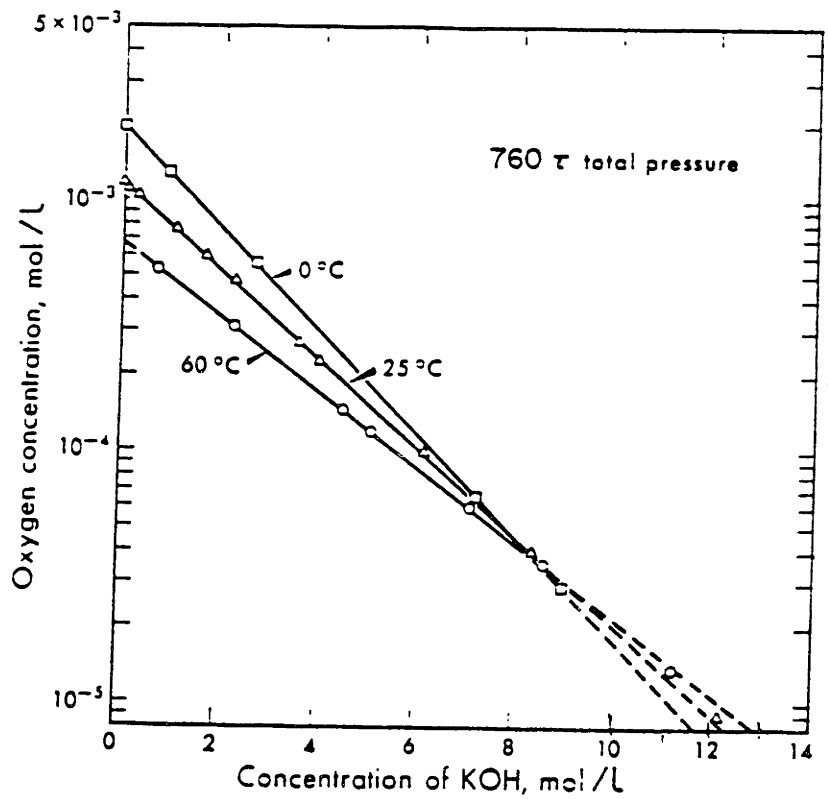

FIG. 2. Solubilities of oxygen in KOH at 0°C, 25°C and 60°C. Data points represent values obtained by Van Slyke method.

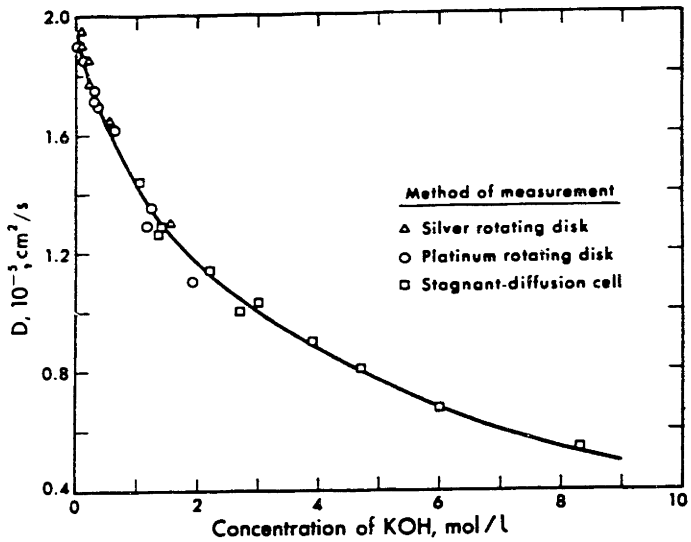

Diffusion coefficients of oxygen in aqueous KOH at 25°C.

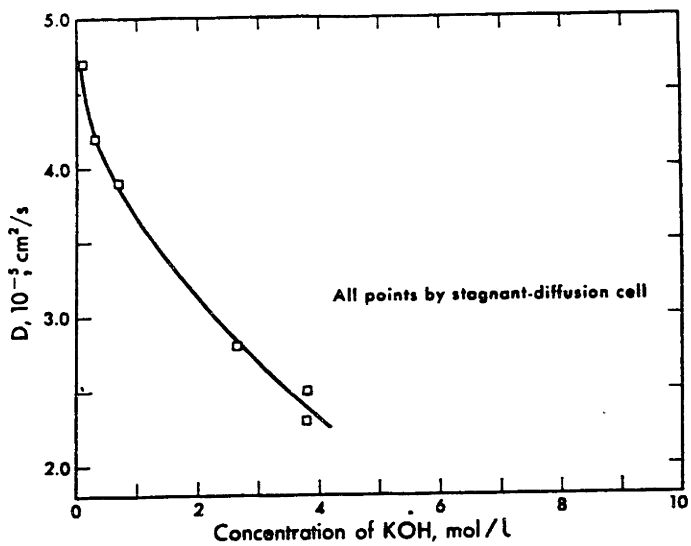

Diffusion coefficients of oxygen in aqueous KOH at 60°C.

Source: [1] CRC Handbook (1990-1991)

Method(s): Unspecified

Solute(s): O_2

Electrolyte(s): H_2SO_4, KOH, $NaOH$

Concentration (Range): varies, see below

Temperature (Range): 310.2 K

Findings: Bunsen coefficient, $10^4\alpha$, at 1 atm

Conc. (mol/l)	H_2SO_4	KOH	$NaOH$
0.938		169	
1.000	209		164
1.030		164	
1.139			155
1.500	189		
1.600	190		
1.844		122	
2.000	177		114
2.105			104
2.122			106
2.135		108	
2.311		102	
2.329		100	
2.500	163		
3.035			74
3.077		79	
3.502		67	
4.071			49
4.848		42	
4.871		37	

Ostwald coefficient, $L = \frac{T}{273.15}\alpha$, where $T = 310.2$

Conc. (mol/l)	H_2SO_4	KOH	$NaOH$
0.9380		0.0192	
1.0000	0.0237		0.0186
1.0300		0.0186	
1.1390			0.0176
1.5000	0.0215		
1.6000	0.0216		
1.8440		0.0139	
2.0000	0.0201		0.0129
2.1050			0.0118
2.1220			0.0120
2.1350		0.0123	
2.3110		0.0116	
2.3290		0.0114	
2.5000	0.0185		
3.0350			0.0084
3.0770		0.0090	
3.5020		0.0076	
4.0710			0.0056
4.8480		0.0048	
4.8710		0.0042	

Bibliography

[1] *CRC Handbook of Chemistry and Physics*, chapter 6. CRC Press, 71st edition, 1990-1991.

[2] P.H. Abelson. Application of fuel cells. *Science*, page 1469, June 1990.

[3] R.E. Andresen. Solubility of oxygen and sulfur dioxide in molten sodium sulfate and oxygen and carbon dioxide in molten sodium carbonate. *Journal of the Electrochemical Society*, 126(2):328–334, February 1979.

[4] A.J. Appleby and F.R. Foulkas. *Fuel Cell Handbook*. Van Nostrand Reinhold, New York, 1989.

[5] Fuel Cell Association. *Fuel Cell News*, December 1989.

[6] R.A. Bajura. A doe perspective on fuel cells. In *Proceedings of the First Annual Fuel Cells Contractors Review Meeting*, number DOE/METC-89/6105, May 1989.

[7] R. Battino. *Solubility Data Series*, volume 7. Pergamon Press, Oxford, 1981.

[8] R. Battino and H.L. Clever. The solubility of gases in liquids. *Chemical Reviews*, 66:395–463, 1966.

[9] R. Battino, T.R. Tettich, and T. Tominaga. The solubility of oxygen and ozone in liquids. *Journal of Physical Chemistry Reference Data*, 12(2):163–178, 1983.

[10] R.P. Belval and M.K. Bergman. The challenge of commercialization: A case study of public power's multi-megawatt fuel cell demonstration. In *1988 Fuel*

Cell Seminar: Program and Abstracts, Washington, DC, October 1988. Courtesy Associates, Incorporated.

[11] C. Bohr. *Z. Physik. Chem.*, 71, 1910.

[12] G.H.J. Broers, M. Schenke, and H.J. Van Bellegoy. Extended abstract. In *28th Mtg. Internt. Soc. Electrochemistry*, pages 313–316, 1977.

[13] J.P. Brown, P. Pietrogrande, T. Tio, and E.S. Wagner. Assessment of centralized medium-sized fuel cell power plants. Technical report, Electric Power Research Institute, November 1985.

[14] G. Bruhn, J. Gerlach, and F. Pawlek. *Zeit. Anorg. Allg. Chem.*, 337, 1965.

[15] E.H. Camera and F.C. Schora. Fuel cells, power for the future. In *Energy and the Environment in the 21st Century*, volume Preprint Volume II, March 1990.

[16] A. Christoff. *Z. Physik. Chem.*, 55, 1906.

[17] M.W. Cook. Ph.d. thesis. Technical Report UCRL-2459, U.S. Atomic Energy Commission, January 1954.

[18] M.W. Cook and D.N. Hanson. *Review of Scientific Instruments*, 28, 1957.

[19] M.W. Cook and D.N. Hanson. Accurate measurement of gas solubility. *The Review of Scientific Instruments*, 28(5):370–374, May 1987.

[20] R.E. Davis, G.L. Horvath, and C.W. Tobias. The solubility and diffusion coefficient of oxygen in potassium hydroxide solutions. *Electrochemica Acta*, 12:287–297, 1967.

[21] C.K. Dyer. A novel thin-film electrochemical device for energy conversion. *Nature*, pages 547–548, February 1990.

[22] M.A. Enayetullah, T.D. DeVilbiss, and J.O'M. Bockris. Activation parameters for oxygen reduction kinetics in trifluoromethane sulfonic acid systems. *Journal of the Electrochemical Society*, 136(11):3369–3376, November 1989.

[23] Bugel et al. The market for fuel cell power plants within municipally owned utilities. Technical Report EPRI GS-6692, Electric Power Research Institute, January 1990.

[24] V.D. Ferraro, D.G. Hegebarth, and R.W. Taylor. *Field Testing of Department of Defense Fuel Cell Power Plants.* Science Applications International Corporation, San Diego, March 1988.

[25] G. Geffcken. *Z. Physik. Chem.*, 49, 1904.

[26] Onsite Fuel Cell Users Group and the Market Business Assessment Task Force. *The GAS POWERCEL National Market Report: Characterization of the Onsite Fuel Cell Market.* December 1985.

[27] K.E. Gubbins and R.D. Walker, Jr. The solubility and diffusivity of oxygen in electrolytic solutions. *Journal of the Electrochemical Society*, 112(5):469–471, May 1965.

[28] J.H. Hildebrand and R.L. Scott. *Regular Solutions.* Prentice-Hall, Inc., Englewood Cliffs, NJ, 1962.

[29] U.B. Holeschovsky. The flooded flow fuel cell: A new approach to fuel cell design. Technical report, Doctoral Thesis Proposal - MIT Dept. of Chemical Engineering, January 1981.

[30] J.H. Keenan, F.G. Keyes, P.G. Hill, and J.G. Moore. *Steam Tables.* John Wiley and Sons, Inc., 1969.

[31] N.E. Khomotuv and E.I. Konnik. *Zh. Fiz. Khim.*, 48, 1974.

[32] K. Kinoshita, F.R. McLarnon, and E.J. Cairns. Fuel cells: A handbook. Technical Report DOE/METC-88/6096, U.S. Department of Energy, Office of Fossil Energy, May 1988.

[33] K. Klinedinst, J.A.S. Bett, J. MacDonald, and P. Stonehart. Oxygen solubility and diffusivity in hot concentrated phosphoric acid. *Electroanalytical Chemistry and Interfacial Electrochemistry*, 57:281–289, 1974.

[34] M.B. Knaster and L.A. Apel'baum. Solubility of hydrogen and oxygen in concentrated potassium hydroxide solution. *Russian Journal of Physical Chemistry*, 38(1):120–122, January 1964.

[35] Olle Lindstrom. Fuel cell markets: A look at economics and installations. *Chemtech*, pages 44–50, January 1989.

[36] C.G. MacArthur. *Journal of Physical Chemistry*, 20, 1916.

[37] C.M. Marschoff and L. Yanes. Niches for commercial utilization of fuel cells in argentina. In *1988 Fuel Cell Seminar: Program and Abstracts*, pages 309–312, Washington, DC, October 1988. Courtesy Associates, Incorporated.

[38] H.P. Meissner. *Pending Patent Application*, November 1989.

[39] H.A.C. Montgomery, N.S. Thom, and A. Cockburn. *Journal of Applied Chemistry*, 14, 1964.

[40] United States Department of Energy. Fuel cell systems program plan: Fy 1990. Technical Report DOE/FE-0106P, U.S. Government Printing Office, October 1989.

[41] Office of Technology Assessment. Marine applications for fuel cell technology – a technical memorandum. Technical Report OTA-TM-O-37, U.S Government Printing Office, February 1986.

[42] G.L. Pollack. Why gases dissolve in liquids. *Science*, 251:1323–1330, March 1991.

[43] J.M. Prausnitz, R.N. Lichtenthaler, and E.G. de Azevedo. *Molecular Thermodynamics of Fluid-Phase Equilibria.* Prentice-Hall, Inc., Englewood Cliffs, NJ, 1986.

[44] Ernest Rala. Fuel cells spark utilities' interest. *High Technology*, December 1984.

[45] Samuel Romano. Fuel cells for transportation. *Mechanical Engineering*, pages 74–77, August 1989.

[46] P. Ruetschi and R.F. Amlie. Solubility of hydrogen in potassium hydroxide and sulfuric acid, salting-out and hydration. *The Journal of Physical Chemistry*, 70(3):718–723, March 1966.

[47] R.L. San Martin. Testimony before the subcommittee on energy research and development, committee on science, space, and technology. Technical report, U.S. House of Representatives, March 1990.

[48] B.R. Scharifker, P. Zelenay, and J.O'M. Bockris. The kinetics of oxygen reduction in molten phosphoric acid at high temperatures. *Journal of the Electrochemical Society*, 134(11):2714–2725, November 1987.

[49] S.K. Shoor, R.D. Walker, and K.E. Gubbins. Salting out of nonpolar gases in aqueous potassium hydroxide solutions. *The Journal of Physical Chemistry*, 73(2):312–317, February 1969.

[50] F. Sissine. Renewable energy - fuel cell technology: Can it compete? In *15th Energy Technology Conference*, February 1988.

[51] Fred Sissine. Fuel cells for electric power production: Future potential, federal role, and policy options. Technical Report 85-523SPR, Congressional Research Service, Science Policy Research Division, January 1985.

[52] S.W. Smith, Vogel W.M., and S. Kopelner. Solubilities of oxygen in fused li_2co_3-k_2co-3. *Journal of the Electrochemical Society*, 129(8):1668–1670, August 1982.

[53] E.L. Stephan, N.S. Hatfield, R.S. Peoples, and H.A.H. Pray. *Battelle Memorial Institute Report*, BMI-1067, 1956.

[54] Karen Trimble and Richard Woods. Fuel cell applications and market opportunities. In *Fuel Cells: Grove Anniversary Symposium '89*, The Netherlands, 1990. Kripps Repro B.V.

[55] G.A. Truesdale, A.L. Downing, and G.F. Lowden. *Journal of Applied Chemistry*, 5, 1955.

[56] D.D. Van Slyke and J.M. Neill. *J. biol. Chem.*, 61, 1924.

[57] R. Wiebe, V.L. Gaddy, and C. Heins. *Ind. Eng. Chem.*, 24, 1932.

[58] L.W. Winkler. *Ber.*, 22, 1889.

[59] A. Yasunischi. *Kagadu Kogaku Rombunshu*, 4, 1978.

[60] C.L. Young. *Hydrogen and Deuterium*, volume 5-6. Pergamon Press, Oxford, 1981.